MONTHLY WEATHER REVIEW
VOLUME 95, NUMBER 2
FEBRUARY 1967

THE MUTUAL VARIATION OF WIND, SHEAR, AND BAROCLINICITY IN THE CUMULUS CONVECTIVE ATMOSPHERE OF THE HURRICANE

WILLIAM M. GRAY

Department of Atmospheric Science, Colorado State University, Fort Collins, Colo.

ABSTRACT

The enhanced cumulus convection in tropical disturbances acts in two opposing ways. In one sense the condensation heat from the cumuli acts to warm the inner portions of the disturbance and induce vertical shear of the horizontal wind through the thermal wind relationship. In the opposite sense the cumuli also act to suppress vertical wind shear by transfer of horizontal momentum within their up- and downdrafts. The operation of this dual or "paradox" role of the cumulus cloud is of fundamental importance for understanding the steady-state dynamics of the hurricane's inner core region and is also hypothesized to be of basic importance in the development of tropical storms and generation of easterly waves.

Observational information and calculations on the radial distribution of baroclinicity and vertical shear collected on 102 individual flight legs (on 19 flight levels) into hurricanes flown by the Research Flight Facility of the U.S. Weather Bureau are presented. The measured baroclinicity in the lower half of the troposphere at the inner 50–70-km. radii is two to three times larger than cylindrical thermal wind balance would require. This baroclinicity may be 50 to 100 times larger in the inner areas of the hurricane than in the easterly wave, yet vertical wind shear in the hurricane may be but one to three times as large.

An extensive discussion is presented on the characteristics of the vertical motion within the hurricane. A steady-state model of mean flow conditions in the inner 80-km. radius based on flight observations and best known surface stress conditions is assumed. Upon this mean vortex motion five sizes of cumulus up- and downdrafts are superimposed with their characteristic eddies and resulting stress. A discussion of the terms in the steady-state equations of motion reveals that sizable amounts of cumulus-produced radial and tangential frictional acceleration is required to satisfy the broadscale mean flow conditions. These cumulus-produced horizontal accelerations account for the imbalance in the thermal wind relationship. Tropical storm development is not viewed as being possible unless the cumulus-induced vertical momentum transfers act in a dominant way to oppose the thermal wind requirement and inhibit increase of vertical wind shear as baroclinicity increases. Vortex development thus requires a continual imbalance of pressure over wind acceleration.

1. INTRODUCTION

The crucial importance of realistically handling the tropical atmosphere and the effects of cumulus convection in treatment of the earth's global circulation has been discussed by the General Circulation Research Groups. Nevertheless, no established methodology for handling the cumulus convective atmosphere has yet been developed. The mutual interactive effects of the cumulus clouds with the synoptic-scale circulations are not well understood for either the general circulation or the tropical storm problem (Yanai [57]).

Recent numerical experiments on tropical storm genesis (Ooyama [36], Kasahara [23], Charney and Eliassen [7], Ogura [35], Kuo [24], Syōno and Yamasaki [52]) have attempted to deal with the cumulus convection by parameterizing the condensation heating of the cumuli in terms of known variables of the larger scale.

These and other model experiments such as Kasahara [22] and Rosenthal [44] have as yet, not considered the possible interactive effects of momentum exchanges associated with the cumulus up- and downdraft elements. But, because of the probable high correlations of cumulus-scale horizontal and vertical wind fluctuations in a vertical

shearing flow, cumulus-scale momentum exchanges may play an equally important or dominant role in the realistic treatment of the cumulus atmosphere (Gray [14]).

With the establishment of the National Hurricane Research Project in 1955, a large quantity of observational information concerning the cumulus convective atmosphere is now available. Certain questions can be answered and inferences drawn as to the physical processes operating on this hitherto incompletely observed convective scale of motion. The intensity of cumulus convection in the tropical storm (particularly near its center) is greater than in any other synoptic-scale storm system. It may be easier to isolate the effects of the cumuli in this system. What we learn about cumulus convection in the inner region of the hurricane may have applicability to other less intense cumulus convective systems such as the easterly wave or squall line. The dynamics of the inner 100-km. radius of the tropical storm where cyclonic circulation is present through the entire troposphere (Riehl [40], Jordan [20]) has yet to be completely studied.

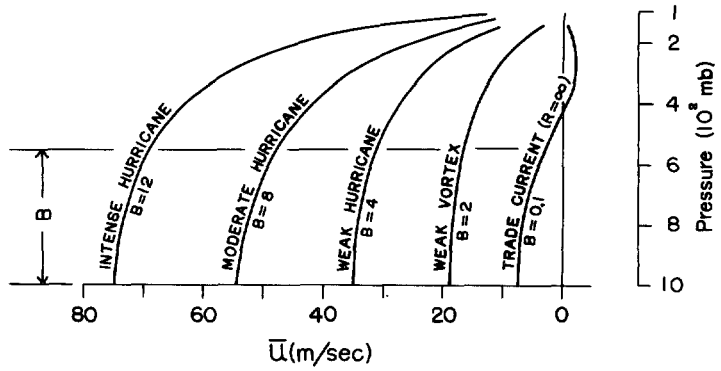

FIGURE 1.—Typical vertical shear of the horizontal wind existing at 40-km. radius in tropical vortices of various intensities and in the usual trade current (radius= ∞). B is the average magnitude of baroclinicity present (° C./100 km. along constant pressure surface) in the lower half of the troposphere (1000–550 mb.) at 40-km. radius under the assumption of cylindrical thermal wind balance. f taken at 15° N.

BACKGROUND

In comparison with the middle latitudes, little horizontal temperature gradient is present in the tropical atmosphere. When large temperature gradients exist, they must be primarily produced by concentrated amounts of cumuli, even though necessary amounts of sensible and latent heat for cumulus buoyancy are received as a dynamic byproduct from the ocean. Advection of heat cannot produce the strong temperature gradients observed in the tropical storm which may exceed wintertime middle-latitude gradients by an order of magnitude. By contrast, middle-latitude gradients of temperature are primarily brought about through meridional advection of radiation-developed temperature differences.

The vertical wind shear near the eye wall in the lower half of the troposphere of the hurricane is only one to three times larger (Hawkins et al. [17]) than the vertical wind shear in a similar layer in the typical easterly wave. Yet the baroclinicity present may be 100 times as large (0.1° C./100 km. vs. 10° C./100 km.—fig. 1). For understanding the progressive development of the hurricane from the pre-existing disturbance, at least two perplexing questions must be answered:

(1) How does it happen that the condensation-developed horizontal temperature gradients in the tropical storm are only slightly reflected by increase of vertical wind shear as occurs with middle-latitude westerly circulations?

(2) How is it possible for cumulus convection (which releases condensation heat on a scale of 2–6 km.) to generate a tropical storm which is of size two to three orders of magnitude larger than the individual cumulus elements?

This paper attempts to offer a physical explanation to the above questions by demonstrating the plausibility of cumulus up- and downdraft (2–6-km. width) momentum transfers acting as a primary mechanism to inhibit increases of vertical wind shear as baroclinicity increases and to couple the upper and lower troposphere and organize the circulation on a larger mesoscale. The cumulus up- and downdrafts also act to inhibit and regulate cross isobaric flow and thereby kinetic energy generation.

Qualitatively the intensification process is envisaged as follows: Differential surface convergence induces differential condensation heating and increase of horizontal temperature gradient between the cumulus and cumulus-free areas. Surface pressure is reduced in the areas of condensation (with assumed stratospheric level of no gradient). An imbalance between pressure and wind acceleration occurs. Although the atmosphere continually tends to adjust itself to gradient wind balance, this adjustment is not instantaneous. In the adjustment to the imbalance of wind and pressure, other accelerations are activated. For the usual increase of horizontal temperature gradient in middle-latitude circulations, an increase of wind shear takes place. But, the vertical momentum transports associated with cumulus-developed baroclinicity in the tropical wave or storm inhibit an increase of the vertical wind shear from acting as the primary mode of adjustment toward gradient balance. The primary adjustment must then come from changes of wind speed and/or curvature of flow. In this sense the cumuli act to "force" a production of wind speed and/or increase of curvature. Cumulus-induced velocity-curvature growth of this type might be termed "cumulus momentum exchange growth."

2. THERMAL WIND EQUATION WITH CURVATURE

NATURAL COORDINATES

With the assumption of frictionless motion and with the hydrostatic approximation, the thermal wind equation in natural coordinates with p as the vertical coordinate

may be written as

$$\left(f+\frac{2V}{R}\right)\frac{\partial V}{\partial p}=-\frac{C}{p}\frac{\partial T}{\partial n}\Big)_p \tag{1}$$

where f=Coriolis parameter
V=horizontal wind speed
R=radius of trajectory curvature which is assumed to be constant with height
p=pressure
C=gas constant
T=virtual temperature of air
n=distance along R, positive to the right of the direction of V in the Northern Hemisphere
$)_p$ denotes differentiation along the constant pressure surface.

In this derivation it is assumed that there is no rotation of the coordinate system with height. The above equation may be more simply written as

$$W_R S_n = B_n \tag{2}$$

where $W_R=\left(f+\frac{2V}{R}\right)$=inertial parameter

$S_n=\frac{\partial V}{\partial p}$=vertical wind shear parameter

$B_n=-\frac{C}{p}\frac{\partial T}{\partial n}\Big)_p$=baroclinicity

If differential condensation heating produces an increase with time of baroclinicity (denoted $\dot{B}_n$), changes in either wind speed ($\dot{V}$), curvature ($\dot{R}$), or wind shear ($\dot{S}_n$) must result (with constant f) as the atmosphere continually attempts to adjust itself to a new thermal wind balance.

If the cumuli act to inhibit changes of S, substantial changes of V and/or R must result to balance even slight horizontal temperature gradient increases. Thus for assumed tropical easterly wave flow with

(1) radius of curvature of 10^3 km.,
(2) wind shear in the lower two-thirds of the troposphere of 6 m./sec.,
(3) mean wind of 5 m./sec. (8 m./sec. at the surface and 2 m./sec. at 400 mb.),

a 0.1° C./100 km. temperature gradient increase with no change of vertical wind shear would require a layer mean wind increase from 5 to ~25 m./sec., or a decrease of the radius of curvature from 1,000 to ~200 km. for continued gradient wind balance (f taken at 20° latitude).

CYLINDRICAL COORDINATES

The complete cylindrical thermal wind equation with origin continually at the center of a vortex,[1] can be written as

$$\left(f+\frac{2u}{r}\right)\frac{\partial u}{\partial p}=-\frac{C}{p}\frac{\partial T}{\partial r}\Big)_p-\frac{\partial F_r}{\partial p}+\frac{\partial}{\partial p}\left(\frac{dv}{dt}\right) \tag{3}$$

[1] The effect of the curvature of the earth may be neglected if consideration is given only to processes at the inner radii ($r<150$ km.).

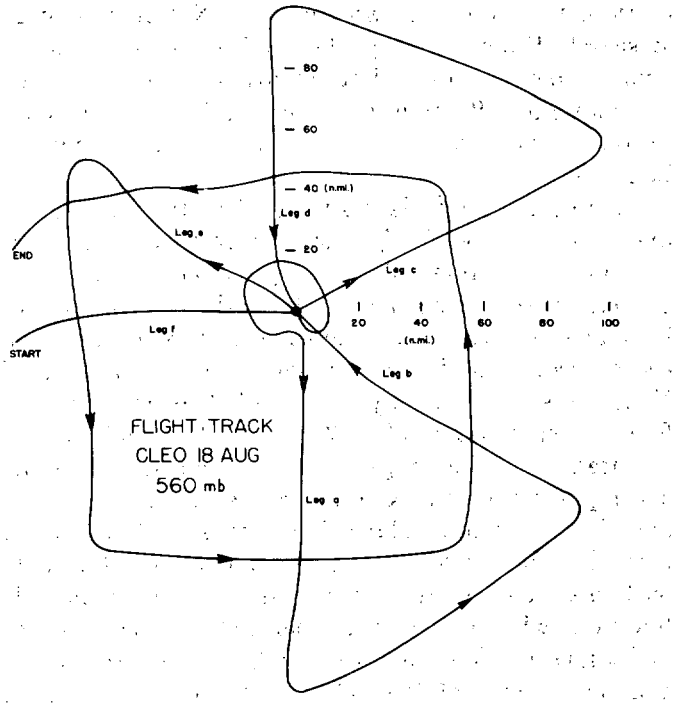

FIGURE 2.—Typical flight track at individual levels.

where r=radius from coordinate origin
u=speed in the tangential or θ direction relative to the moving storm center, positive counterclockwise
v=speed in the radial direction relative to the moving storm center, positive outward
F_r=frictional acceleration in radial direction
$\frac{d}{dt}$=substantial derivative

and other symbols as before.

If we disregard the second and third terms on the right of (3) by assuming steady, frictionless motion, (3) can be written as

$$W_r S = B \tag{4}$$

where $W_r=\left(f+\frac{2u}{r}\right)$

$S=\frac{\partial u}{\partial p}$

$B=-\frac{C}{p}\frac{\partial T}{\partial r}\Big)_p$

If balanced conditions were periodically to prevail at incremental periods following increases of B with no increase of S, u would then be directly related to B.

3. OBSERVATIONAL INFORMATION

To what extent do the meteorological observations support the above hypothesis concerning the importance of vertical cloud-scale momentum transports? The air-

craft flight tracks flown by the National Hurricane Research Project during the 1958–61 seasons (fig. 2 is typical) permit direct determination of W_r and B along the individual flight legs. A calculation of the required vertical wind shear to accompany W_r and B may then be made.

In addition, if it is assumed that the individual leg observations on each flight level were taken over a quasi-constant time interval, an approximation to the tangential average parameters along the storm radius can be made by assigning weighting factors to each radial leg according to its percentage area of representation. Four to seven (usually 5–6) radial penetrations were flown over periods of 4–7 hr. Determination of the required vortex average vertical wind shear $\partial u/\partial p$ to accompany the vortex average measured values of W_r and B for steady, balanced, frictionless flow conditions may thus be made. A direct comparison of calculated with measured vertical wind shear values is possible in five cases when two aircraft operated together at different flight levels. Determination of the degree to which the cylindrical form of the balanced thermal wind equation (4) is applicable to the hurricane vortex may then be made.

Descriptions of the aircraft used, the meteorological instrumentation, the flight tracks flown, and the character of the data collected, etc., have been extensively discussed (Hawkins, et al. [16], Riehl and Malkus [42], Reber and Friedman [39], Colón and Staff *NHRP* [8], [9], Gray [12], [13], [14], Miller [31], LaSeur and Hawkins [25], Gentry [10]). The reader is referred to these for detailed information on the characteristics of the data.

Table 1 lists information concerning 19 flight levels for which individual radial leg and vortex average radial temperature and wind data are available. Table 2 lists observed flight-level vortex average radial adjusted temperature decrease (or temperature gradient along the constant pressure surface) in 18-km. segments from 18 to 90–126 km. In order that truly representative temperature gradients might be obtained, all spot temperatures used were obtained from averaging over 9 km. on either side of the boundary value used. The temperature gradient between radii 36 and 54 km. is thus obtained from the difference of the mean temperature in the radial interval between 45 and 63 km. subtracted from that of the mean temperature in the interval between 27 and 45 km. (fig. 3).

Virtual temperature correction has not been made. Relative humidities are between 80 and 100 percent at the inner radii in the middle and lower troposphere. This would account for a maximum error of 0.2° C. in the temperature gradients. As temperatures are averaged over 18 km., radial gradients of any possible wet-bulb effect on the vortex temperature reading are not thought significant.

The listed vortex average temperature gradients of table 2 are demonstrated to be reasonable if a comparison

TABLE 1.—*Flight Level Information*

Storm	Date	Flight level (mb.)	Radius of data (km.)	Number of flight leg calculations	Approximate maximum wind at flight level (m./sec.)	Approximate central pressure (mb.)	Speed of storm (m./sec.)
Carrie	Sept. 15, 1957	605	18–108	6	42	965	6
	Sept. 17, 1957	690	18–108	6	47	970	6
Cleo	Aug. 18, 1958	810	18–126	5	45	970	7
	do	560	18–126	6	40	970	7
	do	255	18–180	4	20	970	7
Daisy	Aug. 25, 1958	825	18–108	6	32	990	3
	do	555	18–108	6	30	990	3
	Aug. 27, 1958	630	18–144	6	60	940	4
	Aug. 28, 1958	620	18–126	7	52	945	9
Helene	Sept. 24, 1958	635	18–90	6	30	995	5
	Sept. 25, 1958	810	18–90	6	40	980	5
	Sept. 26, 1958	580	18–90	5	60	950	7
	do	270	18–180	4	40	950	7
Donna	Sept. 7, 1960	760	18–108	4	64	945	5
	do	635	18–72	4	60	945	5
Carla	Sept. 6, 1961	905	18–108	6	32	980	6
	do	585	18–108	6	25	980	6
	Sept. 8, 1961	860	18–144	4	42	955	5
	do	720	18–144	4	39	955	5

TABLE 2.—*Vortex average radial temperature decreases along constant pressure surfaces (°C.)*

Storm	Date	Flight level (mb.)	Radius (km.)						
			18–36	36–54	54–72	72–90	90–108	108–126	18–72
Carrie	Sept. 15, 1957	605	3.9	2.1	0.1	1.4	−0.4		6.1
	Sept. 17, 1957	690	.2	2.1	1.8	0	.4		4.1
Cleo	Aug. 18, 1958	810	2.2	1.2	−.1	.1	.3	0.3	3.3
	do	560	3.1	1.9	−.2	.5	.6	1	4.8
	do	255	.1	.7	1.3	1.0	1.0	.2	2.1
Daisy	Aug. 25, 1958	825	1.7	0	−.3	0	0		1.4
	do	555	.8	.4	−.1	−.2	−.1	−.4	1.1
	Aug. 27, 1958	630	2.3	.4	−.3	0	−.1	.1	2.4
	Aug. 28, 1958	620	4.5	1.7	1.2	.7	0	.1	6.4
Helene	Sept. 24, 1958	635	1.5	1.5	.5	.3			3.5
	Sept. 25, 1958	810	−.1	1.9	1.0	.3			2.8
	Sept. 26, 1958*	580	4.9	1.0	0	.7	−.6		5.9
	do*	270	1.3	2.7	1.5	.9	.6		5.5
Donna	Sept. 7, 1960	760	3.4	1.1	1.1	.7			5.6
	do	635	5.5	2.1	.2				7.8
Carla	Sept. 6, 1961	905	1.0	.5	.2	.1	0		1.7
	do	585	.9	.5	.3	.2	−.1		1.7
	Sept. 8, 1961	860	−.2	1.0	.6	.4	0		1.4
	do	720	1.1	2.5	1.3	.5	.2		4.9
Average			2.0	1.3	.5	.4			3.8

*Southern quadrant value taken from 710-mb. flight leg.

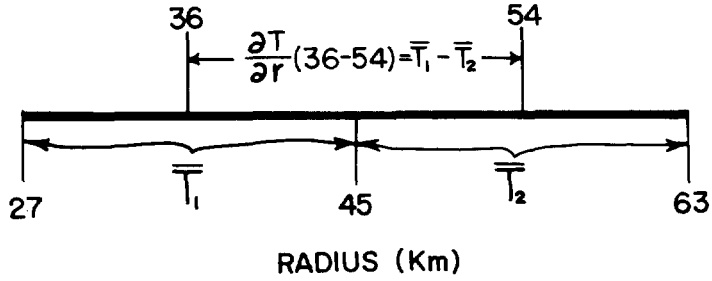

FIGURE 3.—Illustrating method of determining temperature gradient between 36- and 54-km. radii.

is made of the observed layer average temperature gradients with the radial gradients of temperature computed from layer thickness differences.[2]

Table 3 shows a close comparison of observed layer average temperature gradients between radial intervals with the temperature gradients obtained from layer thickness gradients for seven available cases. Hydrostatic consistency was closely approximated. For these reasons the observed 18-km. average temperature gradients are thought to be reliable in the inner area of the hurricane where sizable temperature gradients are present.

Computations of W_r and B terms were made along the radial legs on all the levels listed.[3] A determination was then made of the vertical wind shear which should accompany W_r and B if steady, balanced flow were present.[4] Table 4 lists typical measured values of temperature gradient and resultant S (in m./sec. per 225 mb. or one-quarter of the troposphere) for gradient balance along radial leg increments on each of the six flight legs of hurricane Cleo at 560 mb. on August 18, 1958. Large variation of ΔT and S are present. The computed vertical shears ranged up to 23 m./sec. per 225 mb. Computations on this level are closely representative of the results obtained on the other individual radial legs.

The area weighted vortex average computed shears in the inner two 18-km. segments for Cleo at 560 mb. were 15 and 8 m./sec. per 225 mb. Yet the vortex average observed wind shears between 810 and 560 mb. for the same radial segments were but 2.3 and 3.5 m./sec. per 225 mb.

Table 5 summarizes results of vortex average calculated vertical wind shear for the highest 36-km. radial segments on 17 middle and lower troposphere levels. Wind shears are given in percentage (or ratio) of amount of shear per 225 mb. to layer average wind speed. Percentage vertical wind shear is defined as

$$\text{percentage shear}=\frac{u_b-u_t}{\bar{u}}\times 100 \qquad (5)$$

where u_t = tangential velocity at top of 225-mb. layer
u_b = tangential velocity at bottom of 225-mb. layer
$\bar{u} = \frac{1}{2}(u_b+u_t)$

Calculated shear as high as 37 percent of the observed mean wind per 225 mb. was obtained. Even though vortex averages were taken, unrealistically high computed percentage shear was obtained at the inner radii. Flight observations have shown, however, that measured wind shears in the lower half of the troposphere at the inner radii of the hurricane are considerably smaller. Hawkins [17] has constructed a nomogram of vertical wind shear obtained from available hurricane flight data of 1957–58. This diagram shows wind shear through the entire lower half of the troposphere (surface to 550 mb.) within radii of 60–80 km. to average but 10 percent of the mean wind speed (3–4 m./sec. per 450 mb. or 5 percent per 225 mb.). Flight observations since 1960 have further substantiated Hawkins' data.

Table 6 lists ratios of percentage vortex average calculated shear to assumed vertical shear of 5 percent per 225 mb. for the 17 middle and lower tropospheric levels. In the radial segments between 18 and 36 km. and between 36 and 54 km. this ratio averages 4.4 and 3.3, respectively. This is 4.4 and 3.3 times larger than Hawkins' wind shear nomogram.

[2] Layer mean temperature was obtained by averaging at the top and bottom.

[3] The relative wind with respect to the moving vortex center was used in the tangential average or symmetric vortex considerations. A small percentage correction to the listed relative tangential wind (i.e., u) was made to compensate the Doppler-determined winds or ocean particle movement (see Appendix).

[4] Because radii diverge the $\left(f+\frac{2u}{r}\right)$ term was calculated as $\overline{f}+\frac{2\bar{u}}{\Delta r}\ln\frac{r_{2i}}{r_{1i}}$ where Δr is a 9-km. interval and r_{2i}, r_{1i} are the outer and inner radii, respectively. $\bar{u}$ is the average value of u over a 9-km. radial interval.

TABLE 3.—*Comparison of vortex average observed and computed temperature gradients*

Storm	Date	Between pressure levels (mb.)	Radius (km.)	Observed temperature gradient (° C.)	Computed temperature gradient (° C.)
Cleo	Aug. 18, 1958	810–560	18–54	3.7	4.0
	do	560–255	18–90	3.6	4.0
Daisy	Aug. 25, 1958	825–555	18–54	1.4	1.4
Helene	Sept. 26, 1958	580–270	18–90	7.0	7.8
Donna	Sept. 7, 1960	760–635	36–72	2.2	1.7
Carla	Sept. 6, 1961	905–585	18–72	1.7	2.0
	Sept. 8, 1961	860–720	18–72	3.2	4.4
Average				3.3	3.6

TABLE 4.—*18-km. incremental individual radial leg temperature gradients (° C.) and calculated vertical wind shear (m./sec. per 225 mb.—parentheses) for 560-mb. flight level of Cleo Aug. 18, 1958.*

Radius (km.)	Storm quadrant of radial flight track (see fig. 1)						Area weighted vortex average
	NE	SE	S	W	NW	N	
18–36	2.5(7.4)	3.6(13.1)	2.9(12.6)	2.8(23.4)	3.0(15.5)	2.9(16.9)	3.1(14.8)
36–54	2.0(6.8)	1.8(5.9)	2.2(6.8)	2.0(10.4)	2.3(7.4)	1.0(9.9)	1.9(7.8)
54–72	−.4(−2.0)	.1(.7)	−.6(−3.6)	.2(1.1)	−.2(−1.3)	−.2(−1.1)	−.2(−1.0)
72–90	.6(4.1)	.3(2.2)	.9(6.5)	.8(5.6)	.1(.8)	.4(3.2)	.5(3.7)
90–108	1.0(8.1)	.3(3.1)	.4(4.1)	0 (0.0)	.7(6.5)	.9(8.3)	.6(5.0)
108–126	.2(1.8)	.1(1.2)	.3(−2.7)	−.9(−9.5)	.1(12.2)	.5(5.8)	.1(1.5)
126–144	.1(1.1)	−.9(−9.0)	.2(2.2)	−9.5(−6.5)		.1(1.3)	

TABLE 5.—*Calculated percentage vertical wind shear per 225 mb. for highest 36-km. radial intervals*

Storm	Date	Level (mb.)	Radius (n. mi.)	Average percentage vertical wind shear per 225 mb.
Carrie	Sept. 15, 1957	605	18–54	31
	Sept. 17, 1957	690	36–72	22
Cleo	Aug. 18, 1957	810	18–54	12
	do	560	18–54	35
Daisy	Aug. 25, 1958	825	18–54	12
	do	555	18–54	13
	Aug. 27, 1958	630	18–54	6
	Aug. 28, 1958	620	18–54	19
Helene	Sept. 24, 1958	635	18–54	37
	Sept. 25, 1958	810	36–72	36
	Sept. 26, 1958	580	18–54	13
Donna	Sept. 7, 1960	760	18–54	6
	do	635	18–54	15
Carla	Sept. 6, 1961	905	18–54	13
	do	585	18–54	34
	Sept. 8, 1961	860	18–54	5
	do	720	18–54	30
Average				20

TABLE 6.—*Ratio of calculated to an assumed vertical wind shear of 5 percent per 225 mb.*

Storm	Date	Level (mb.)	Radius (km.)		
			18–36	36–54	54–72
Carrie	Sept. 15, 1957	605	9.4	3.2	0.4
	Sept. 17, 1957	690	.8	5.4	3.2
Cleo	Aug. 18, 1958	810	3.6	1.4	−.2
	do	560	9.4	4.6	−.6
Daisy	Aug. 25, 1958	825	10.0	−.4	−2.6
	do	555	2.8	2.6	−1.0
	Aug. 27, 1958	630	1.6	.6	−1.4
	Aug. 28, 1958	620	4.4	3.2	4.2
Helene	Sept. 24, 1958	635	7.4	7.6	2.3
	Sept. 25, 1958	810	−.8	8.8	5.3
	Sept. 26, 1958	580	3.8	1.4	0
Donna	Sept. 7, 1960	760	1.6	.8	1.6
	do	635	3.6	2.2	.4
Carla	Sept. 6, 1961	905	3.0	2.1	.8
	do	585	7.6	6.0	4.4
	Sept. 8, 1961	860	−.8	1.8	1.2
	do	720	7.4	4.4	3.2
Average			4.4	3.3	1.3

TABLE 7.—*Ratio of calculated to observed percentage wind shear per 225 mb.*

Storm	Date	Between pressure levels (mb.)	Radius (km.)		
			18–36	36–54	54–72
Cleo	Aug. 18, 1958	810–560	25/10	22/11	9/3
Daisy	Aug. 25, 1958	825–555	32/6	6/−7	−9/−10
Donna	Sept. 7, 1960	760–635	13/−2	8/8	5/1
Carla	Sept. 6, 1961	905–585	26/19	20/12	13/21
Carla	Sept. 8, 1961	860–720	16/6	16/12	11/13
Average			22/8	13/7	6/6

Five cases are available in which the aircraft operated simultaneously at different levels in the lower troposphere so that direct measurement of actual wind shear could be made. Table 7 lists a comparison of computed and observed percentage vertical wind shears per 225 mb. For the inner two 18-km. radial segments the ratio of computed to observed shear was nearly three and two, respectively. There seems to be no question that the observed vertical wind shears at the inner radii may be one-half to one-third the value of the computed shears obtained from the horizontal temperature gradients. Why should this happen?

A complete evaluation of equation (4) could be accomplished in five cases for which vertical shear was measured. Table 8 portrays computed values of W_rS and B for these cases. When B is larger or smaller than W_rS, then an excess (B_{ex}) or deficit ($-B_{ex}$) of baroclinicity above or below that required for balanced flow is hypothesized to be present. Thus

$$B_{ex}=B-W_rS \tag{6}$$

It is evident that excess baroclinicity of quite pronounced magnitudes is continuously present at the middle and lower tropospheric levels in the inner radii.[5] Values

[5] Numerous reconnaissance missions at the middle and lower tropospheric levels into the inner area of typhoons have also reported sharp increases of horizontal temperature right before and during entry to the eye-wall clouds.

TABLE 8.—*Layer average calculations of B, W_rS, and B_{ex} (units 10^{-6} cm.^{2}/gm.)*

Storm	Date	Between pressure levels (mb.)	Radius (km.)								
			18–36			36–54			54–72		
			B	W_rS	B_{ex}	B	W_rS	B_{ex}	B	W_rS	B_{ex}
Cleo	Aug. 18, 1958	810–560	6.5	1.9	4.6	3.6	2.8	0.8	−1.4	0.6	−2.0
Daisy	Aug. 25, 1958	825–555	2.9	.9	2.0	.5	−.1	.6	−.5	−.3	−.2
Donna	Sept. 7, 1960	760–635	9.9	1.2	8.7	3.5	3.8	−.3	1.3	.4	.9
Carla	Sept. 6, 1961	905–585	2.3	1.1	1.2	1.1	.6	.5	.5	.4	.1
	Sept. 8, 1961	860–720	.9	.3	.6	3.4	2.0	1.4	2.0	1.4	.6
Average			4.5	1.1	3.4	2.4	1.8	.6	.4	.5	−.1

of B_{ex} were frequently as large or larger than the W_rS and B terms themselves. An assumption of frictionless, gradient wind balance would be significantly in error in these areas where large B_{ex} exists.

It is surprising that the cylindrical thermal wind relationship should fail to describe the motion of the inner areas of the hurricane by margins as large as 200 to 400 percent. The large positive B_{ex} in the lower troposphere is consistent with an excess of pressure gradient over measured winds. In an earlier study, the author (Gray [12]) noted a vortex average excess of pressure over wind acceleration in a similar data sample.

LOWER TROPOSPHERIC BAROCLINICITY AND CLOUD ENTRAINMENT

Although the most intense baroclinicity in the developed storm is found at levels between 500 and 200 mb., table 2 shows that large baroclinicity is also present in the lower half of the troposphere. This is consistent with the facts that (1) nearly all condensation heating occurs below 500 mb., (2) a significant percentage of shallow cumulus convection is also present, and (3) observed magnitude of the deep vertical draft velocities and time scale of the deep cumulus cell is possible only if significant amounts of entrainment and turbulent mixing are taking place on the cloud boundaries.

Were "undilute" cumulus ascent hypothesized for the lower part of the troposphere, then vertical draft velocity would have to be two to three times larger than, and cell lifetime one-half to one-third the size they are observed to be (Byers and Braham [4], Gray [13], Simpson et al. [53], Senn et al. [49]).[6] By allowing shallow cumulus convection and some entrainment and turbulent mixing of the cumuli, substantial baroclinicity may be developed in the lower atmosphere. Ackerman [1] has measured liquid water contents within cumulus clouds along a number of the flight levels here discussed, and found amounts below those required for undilute ascent.

Cumulus intensity is greatest in and near the eye-wall area of the hurricane. It is in this region that the direct dynamic influences of the cumuli are more clearly evident and can be more easily isolated from the other parameters. The above envisaged cumulus momentum exchanges are also acting within other areas and circulations, but their relative importance is smaller and present instrumental limitation does not allow for accurate isolation and assessment.

The following sections of this paper will attempt to explain the excess baroclinicity as a plausible consequence of the characteristic dynamical process associated with the hurricane's cumulus momentum exchanges.

[6] If virtual temperature difference between cumulus cloud and environment averaged 2° C. through the layer from 950 to 500 mb. (moist ascent from 950 to 500 mb. in the West Indies summertime sounding requires 2.8° C. average difference of convective and environment virtual temperature), then the magnitude of the vertical draft at 500 mb. and the draft lifetime would be approximately 20 m./sec. and 5 min., respectively. Higher draft magnitudes would occur at 400 and 300 mb.

4. CHARACTER OF VERTICAL MOTION AND STRESS IN THE HURRICANE

Qualitative inspection of hurricane radar echo information has shown the heavy liquid water (and undoubtedly the primary vertical motion) to be concentrated in the selective cumulus cloud areas which may occupy but 5–20 percent of the hurricane's inner area (Jordan [20], Malkus [30], Malkus et al. [29], Riehl and Malkus [42], Colón and staff NHRP [8], [9], Ackerman [1], Gentry[10], and Simpson et al. [53]). The author (Gray [13]) has made an investigation of the width and magnitude of hurricane cumulus drafts. Radar observational studies of the motion of hurricane precipitation echoes have been made by Senn and Hiser [48], Senn and Low [47], Senn et al. [49], [50], [51], Watanabe [56], and others. The above and additional observational evidence allows an inductive determination of the character of the vertical motion at the inner radii of the hurricane.

From the work of Riehl and Malkus [41], [42], and Malkus [30], it is concluded that the vertical motion of primary significance occurs within cumuli which often penetrate into the upper half of the troposphere. No dynamically significant vertical motion is believed to occur in the clear air or within the layered or stratus clouds between the cumuli. The lifetime of the deep cumulus cell averages 30 min. This cell life-cycle is pictured as having two periods, the first of 10–15 min. duration when the vertical motion is predominantly upward, and a similar later period when the motion is predominantly downward. This is in agreement with the cell life-cycle envisaged by Byers and Braham [4]. The magnitude and width of the up- and downdrafts are similar. The mass circulation through the hurricane results from a more intense and slightly greater number of updrafts than downdrafts.[7] This mean vertical motion or mass-circulation through the storm system is not representative of the average absolute vertical motion occurring within the system if typical up- and downdrafts have a magnitude of 5–10 m./sec.

MOMENTUM EXCHANGES AND STRESS ASSOCIATED WITH THE CUMULUS DRAFTS

In a previous observational paper on hurricane dynamics, the author (Gray [14]) stressed the importance of vertical momentum exchanges associated with the correlation of cumulus-scale wind components. By performing space averaging, the wind could be separated into space-determined mean and cumulus-sized eddy components. The measured cloud-scale horizontal and vertical eddies (u', v', ω') were of magnitude 5–10 m./sec. and the components were often highly correlated. Sizable horizontal accelerations could result from vertical gradients of the cumulus-induced stress.

The sign of the $u'\omega'$ correlation was typically negative

[7] The downdraft is established by frictional drag of the falling, strongly concentrated, heavy raindrops. This is assumed to be possible without invoking an evaporation-cooling mechanism.

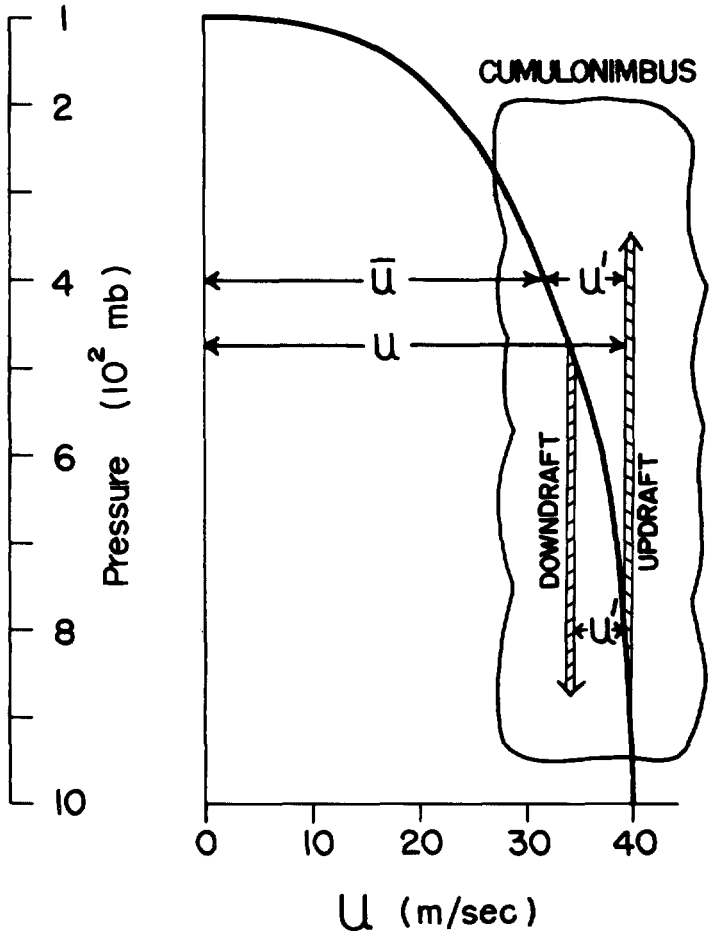

FIGURE 4.—Portrayal of how the horizontal velocity within the deep cumuli can be different from the velocity of the surrounding cumulus-free area if large vertical wind shear is present. The tangential velocity at any level within the draft (u) may be significantly different (u') from the horizontally averaged tangential wind ($\bar{u}$) surrounding the cumuli.

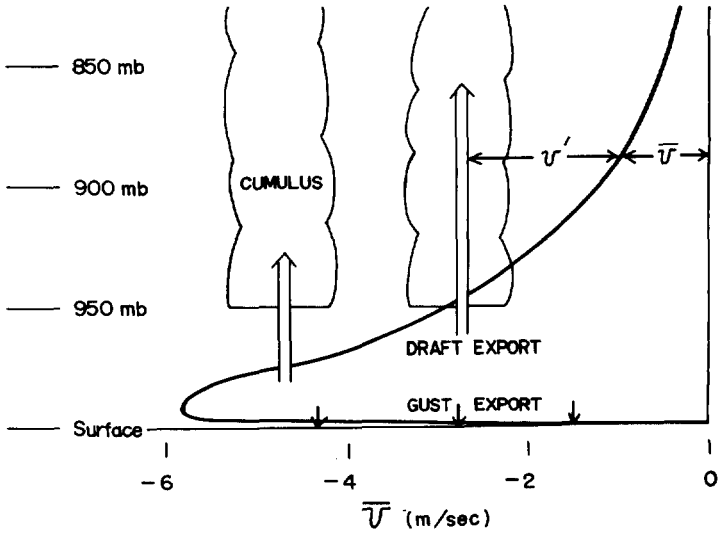

FIGURE 5.—Illustrating how cumulus updrafts from within the lower inflow layer can produce at higher levels negative radial velocities (v') significantly greater than the mean radial velocities ($\bar{v}$) surrounding the cumulus. Typical exports of momentum out of the inflow layer by the gust (below) and the draft (above) processes are also shown.

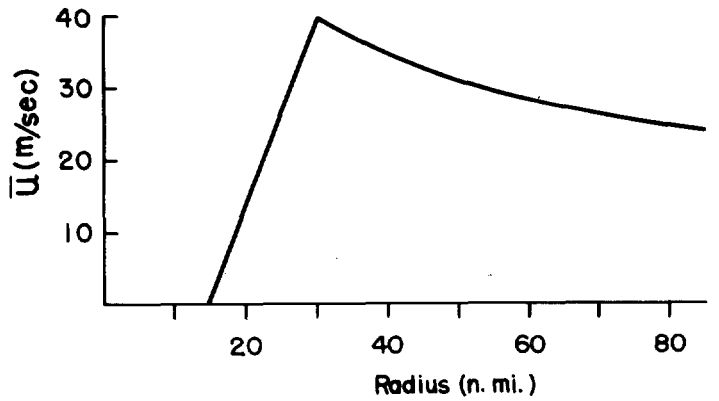

FIGURE 6.—Assumed radial profile of mean tangential wind ($\bar{u}$).

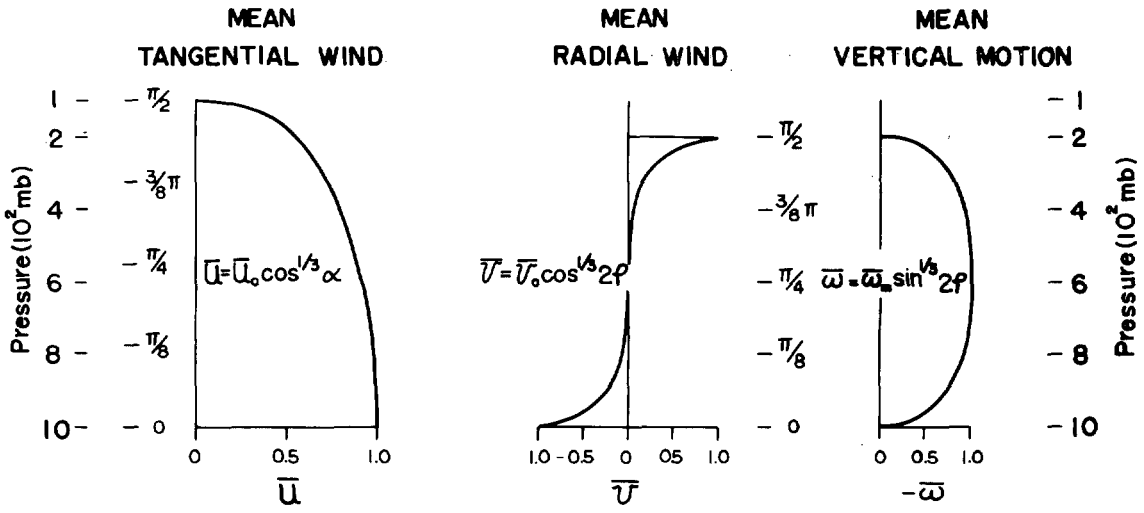

FIGURE 7.—Assumed vertical dependence throughout the troposphere of the mean tangential ($\bar{u}$), radial ($\bar{v}$), and vertical wind ($\bar{\omega}$).

in the middle levels indicating upward vertical momentum transport as is *required by cumulus penetration through a layer where the mean wind decreases with height.* The large horizontal momentum in the lower levels is carried by the updraft to higher levels. A resulting higher horizontal wind speed is present within and surrounding the updraft. The opposite process will be in operation with the downdraft (fig. 4). A high correlation of $v'\omega'$ should also exist in the lower layers where the vertical gradient of radial wind is large (fig. 5). Radar evidence is available (previously cited) which shows that the "hard core" echoes often have horizontal velocities considerably different from those of the surrounding cumulus-free air in the hurricane and also within mid-latitude cumulonimbi (Newton and Newton [33] and Newton [34]). Byers and Battan [5] and Malkus [26] have previously discussed the effects of vertical wind shear on cumuli.

In order to gain more insight into the internal dynamics of the inner area of the hurricane and to explain quantitatively the lack of thermal wind balance as a plausible consequence of the cumulus vertical momentum transports, a symmetric vortex flow pattern for this area based on recent flight observations will be assumed and discussed in the following three sections.

5. ASSUMED VORTEX MODEL

A symmetric steady-state vortex flow pattern is now arbitrarily specified. Upon this mean flow pattern a distribution of three sizes of cumulus convection will be superimposed. Plausible cloud-scale wind fluctuations associated with these cumuli will also be assumed. This complete specification of the mean flow and cumulus-scale wind eddies will allow for calculations of the frictional and other terms in the equations of motion. The following parameters are specified to represent the conditions within the inner 80-km. radius of the moderate, moving hurricane with cumulus convection concentrated in eye-wall clouds at 33 km.

a. Tangential Wind in Horizontal. In agreement with Riehl [43], a relationship

$$\overline{u}r^x=\text{constant} \tag{7}$$

is taken as the functional form of the mean tangential wind ($\overline{u}$) with radius r . $x=-1$ for radii from 15 to 30 km., and 0.5 for radii beyond 30 km. (fig. 6). For the data sample here presented, Riehl [43] has shown that $x=0.5$ closely fits a majority of the radial wind profiles beyond the radius of maximum winds. Maximum wind is assumed to be 40 m./sec. at 30-km. radius.

b. Tangential Wind in Vertical. The vertical distribution of the mean value of u is taken to be given as

$$\overline{u}=\overline{u}_0 \cos^{1/3} \alpha \tag{8}$$

where $\overline{u}_0$ is the mean wind at the surface, and $\alpha=0$ and $\pi/2$ at 1000 and 100 mb., respectively, as shown by the diagram on the left of figure 7. α and φ to follow are linear functions of pressure.

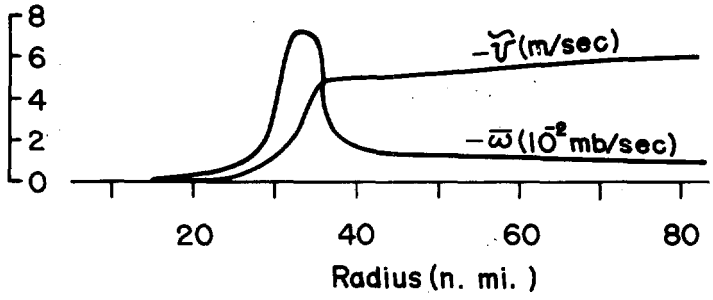

FIGURE 8.—Radial distribution of the average inward radial speed ($\tilde{v}$) in the lowest 100 mb. and upward vertical speed at 900 mb. ($-\bar{\omega}$) which results from tangential wind and stress assumptions.

c. Radial Distribution of Radial Wind. Following Palmén and Riehl [38], Malkus and Riehl [28], and Miller [32], we assume that the surface stress ($\tau_{\theta p_0}$) varies according to the usual relationship

$$\tau_{\theta p_0}=\rho_0 K \overline{u}_0^2 \tag{9}$$

where K is an arbitrarily specified exchange coefficient for gust-scale momentum transfer at the ocean surface. This constant is assigned the value 2.5×10^{-3}, and ρ_0 is the surface density. If 90 percent of the interface-induced stress is assumed to dissipate in the lowest 100 mb., the average tangential frictional acceleration in the lowest 100 mb. (F_θ) is assumed to be given by the relation

$$\tilde{F}_\theta=(0.9)g\frac{\tau_{\theta z_0}}{\Delta p} \tag{10}$$

where g is the gravitational acceleration, Δp a 100-mb. thickness, and $\sim$ denotes vertical averaging.

Given $\tilde{F}_\theta$, the average radial velocity in the lowest 100 mb. of the steady-state symmetrical hurricane is very closely determined from the cylindrical tangential equation of motion

$$\left(-\tilde{v}\tilde{\zeta}_a-\tilde{\omega}\frac{\partial\overline{u}}{\partial p}+\tilde{F}_\theta=0\right)$$

by the relationship

$$\tilde{v}\approx(\tilde{F}_\theta/\tilde{\zeta}_a) \tag{11}$$

where $\tilde{\zeta}_a$ is the average absolute vorticity within this layer depth. The negligible vertical shear of $\overline{u}$ in the lowest 100 mb. allows the $\widetilde{\omega\partial u/\partial p}$ term to be neglected. The radial distribution of $\tilde{v}$ in the lowest 100 mb. and the resulting mean upward speed ($-\bar{\omega}$) at 100 mb. above the surface level is portrayed in figure 8. The radial distribution of $\tilde{v}$ is in agreement with observational evidence of Hughes [19] and others.

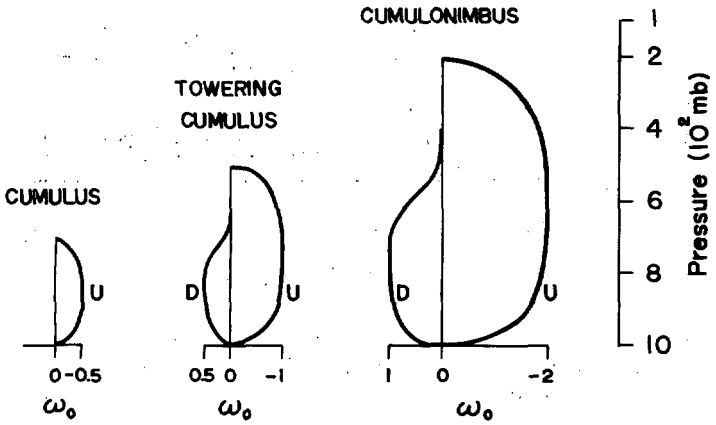

FIGURE 9.—Portrayal of the relative magnitude and depth of the five classes of assumed cumulus updrafts (U) and downdrafts (D).

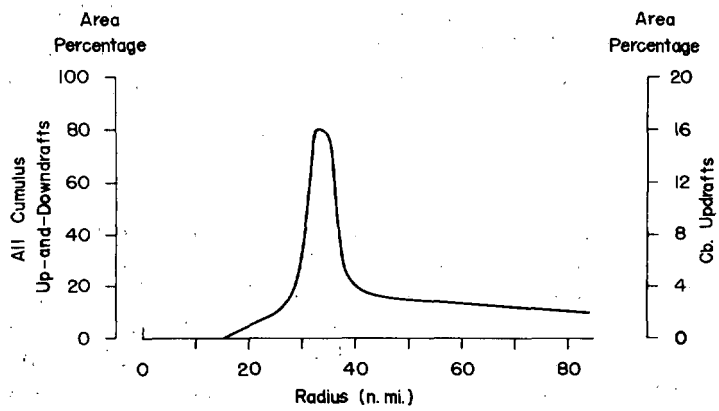

FIGURE 10.—Radial distribution of the percentage of area at each radius which is occupied by *each* class of cumulus up- and downdrafts (scale on right), and the total percentage of area which is occupied by all five classes of cumulus up- and downdrafts (scale on left).

d. Radial Wind in Vertical. The mean radial wind is assumed to vary with height at each radius as shown by the center diagram in figure 7. The functional form of this is given by

$$\bar{v}=\bar{v}_0 \cos^{1/3} 2\varphi \qquad (12)$$

with $\varphi=0$ and $\pi/2$ at 1000 and 200 mb. $\bar{v}_0$=the mean surface radial wind and was determined from frictional drag considerations in *c* above.

e. Vertical Wind. The mean vertical motion at each radius is assumed to vary as

$$\bar{\omega}=\bar{\omega}_m \sin^{1/3} 2\varphi \qquad (13)$$

as shown by the diagram on the right in figure 7. ω_m is the mean vertical velocity at 600 mb. at any radius, $\varphi=0$ and $\pi/2$ at 1000 and 200 mb., respectively.

f. Cloud Distributions and Up- and Downdrafts. A variety of cumulus cloud sizes exists in the tropical storm. It is difficult to deal with all of these. For simplicity it will be assumed that there are three typical cumulus sizes each existing in equal percentage area amounts. The effect of layered or stratus type clouds will be assumed to be negligible. The vertical motion within the cumuli will be given by the basic equation

$$\omega=\omega_0 \sin^{1/3} 2\varphi \qquad (14)$$

The three types of cumuli assumed are:

(1) small cumuli (Cu) which extend from 950 to 700 mb. Maximum upward speed (at 825 mb.) is taken to be $0.5\omega_0$, no downdrafts present. $\varphi=0$ and $\pi/2$ at 1000 and 700 mb.

(2) towering cumuli (TWG Cu) which extend from 950 to 500 mb. Maximum upward speed is $1.0\omega_0$ and downdrafts $0.5\omega_0$. $\varphi=0$, $\pi/2$ at 1000 and 500 mb. respectively for the updraft and 0 and $\pi/2$ at 1000 and 700 mb. for the towering cumulus downdrafts.

(3) cumulonimbi (Cb) which extend to the 200-mb. level. Maximum updrafts and downdrafts are 2.0 and $1.0\omega_0$, respectively, where $\varphi=0$ and $\pi/2$ at 1000 and 200 mb. for the updraft and 0, $\pi/2$ at 1000 and 500 mb. for the downdraft.

The magnitude of ω_0 is specified such that the maximum speeds of the Cb updrafts, Cb downdrafts, and TWG Cu updrafts and Cu updrafts are always 8, 4, and 2 m./sec., respectively, or 4.8, 3.4, and 1.7 m./sec. at 900 mb. The upward circulation through the vortex is carried by the Cb updrafts. The Cb downdrafts are balanced by the TWG Cu updrafts, the TWG Cu downdrafts by the small Cu updrafts.

Figure 9 portrays the relative magnitude of these five classes of cumulus up- and downdraft patterns. Figure 10 shows the percentage area of Cb updrafts and of each of the other types of cumulus up- and downdraft as a function of radius and also the total percentage area taken up by all five classes of updraft and downdraft. The magnitude of the draft speeds and mean vertical circulation determine these area percentages.

The above fits basic observational flight evidence of the characteristics of the typical moderate hurricane circulation which is moving with the cumulus convection concentrated in its center. Mass balance is present at each radius. The cumulonimbi extend to the upper troposphere and the mass inflow and outflow circulation is concentrated in the lowest 100 mb. and at 200 mb., respectively.

6. ASSUMED CUMULUS-INDUCED WIND EDDIES

The above specification of cumulus up- and downdrafts which are superimposed upon the mean flow conditions (in which vertical shear is present) must of necessity require that the winds within the cumuli be different from the mean winds surrounding the clouds. As shown in figures 4 and 5, the horizontal momentum in the lowest layers can be advected upward within the cumulus updraft to produce a component wind at a higher level which is significantly different from the mean wind component surrounding the cumuli. These cumulus-induced component wind variations will henceforth be called eddy winds.

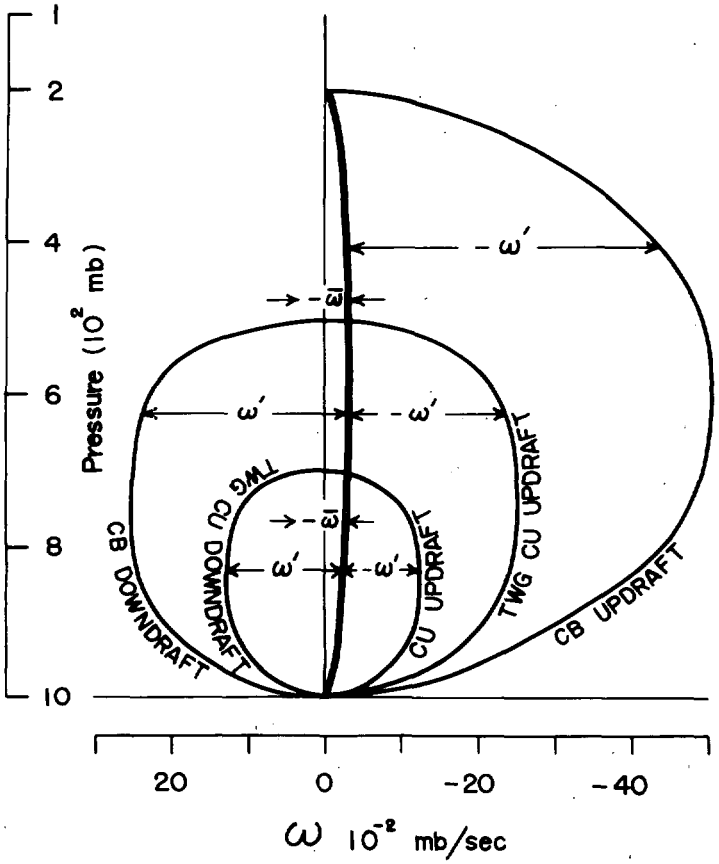

FIGURE 11.—Portrayal of the relative magnitude of the five assumed classes of cumulus up- and downdrafts for average conditions between 30- and 50-km. radii, and how each updraft and downdraft can be significantly different ($\pm\omega'$) from the mean vertical motion ($-\bar{\omega}$) through the system. [Cumulonimbus (Cb), Towering Cumulus (TWG Cu) and Cumulus (Cu)].

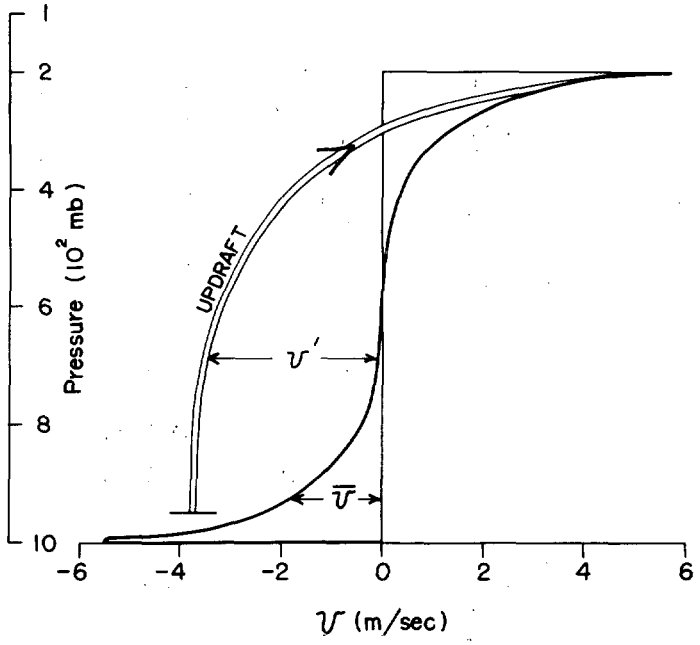

FIGURE 12.—Vertical distribution of the assumed radial eddy wind (v') which results from a cumulonimbus updraft which penetrates to 200 mb. Radial eddy wind $v'=(v_i-\bar{v})\cos\varphi$.

VERTICAL EDDY WIND (ω')

With the previously specified functional form of ω with height, the magnitude of the typical vertical eddy wind associated with each cumulus up- and downdraft is portrayed in figure 11 and defined as

$$\omega'=\omega-\bar{\omega} \tag{15}$$

where $\bar{\omega}$ and ω have been previously specified in sections 5*e* and 5*f*.

The mean upward vertical speed ($-\omega$) is accounted for by the speed of the Cb updrafts multiplied by the area made up by the Cb's (average approximately 6.5 percent between 30- and 50-km. radii). The mean vertical circulation through the system is thus but a small fraction of a m./sec. and the vertical eddy wind is closely approximated by the velocity within the cumuli ($\omega'\sim\omega$).

TANGENTIAL EDDY WIND (u')

The tangential eddy wind is produced by the cumuli advecting larger tangential momentum from below in the updraft and smaller tangential momentum from above in the downdraft (fig. 4). The Cb updrafts are most effective in this transfer because they penetrate through the greatest vertical shear. At the upper levels the difference between the tangential wind and the surrounding flow can be appreciable. At these levels large horizontal mixing must be occurring. The tangential eddy is arbitrarily specified as

$$u'=\bar{u}_0(1-\cos^{1/3}\alpha)M_\theta \tag{16}$$

where $u_0(1-\cos^{1/3}\alpha)$=the maximum eddy wind which would result from undilute ascent from the surface; $\alpha=0$ and $\pi/2$ at 1000 and 100 mb.; and M_θ=coefficient of mixing which is taken to be proportional to $\cos^{1/3}\varphi$. The greatest mixing is thus assumed to occur at the upper levels of each cloud. Then

$$u'=u_0(1-\cos^{1/3}\alpha)\cos^{1/3}\varphi,$$

where $\varphi=0$, and $\pi/2$ at 1000 and 200 mb. in the Cb updrafts, 1000 and 500 mb. in the Cb downdrafts and TWG Cu updrafts, and 1000 and 700 mb. in the TWG Cu downdrafts and Cu updrafts.

A vertical portrayal of the tangential eddy wind which results from a Cb updraft is shown in the upper left diagram of figure 13. Smaller horizontal eddies would occur for the four other classes of cumulus up- and downdrafts.

RADIAL EDDY WIND

The radial eddy is produced in a similar manner as the tangential eddy. However, the larger radial than tangential wind shear in the lower levels requires that the radial eddy (v') and the radial mixing be larger at these levels. The radial eddy wind is arbitrarily specified for levels above 950 mb. as

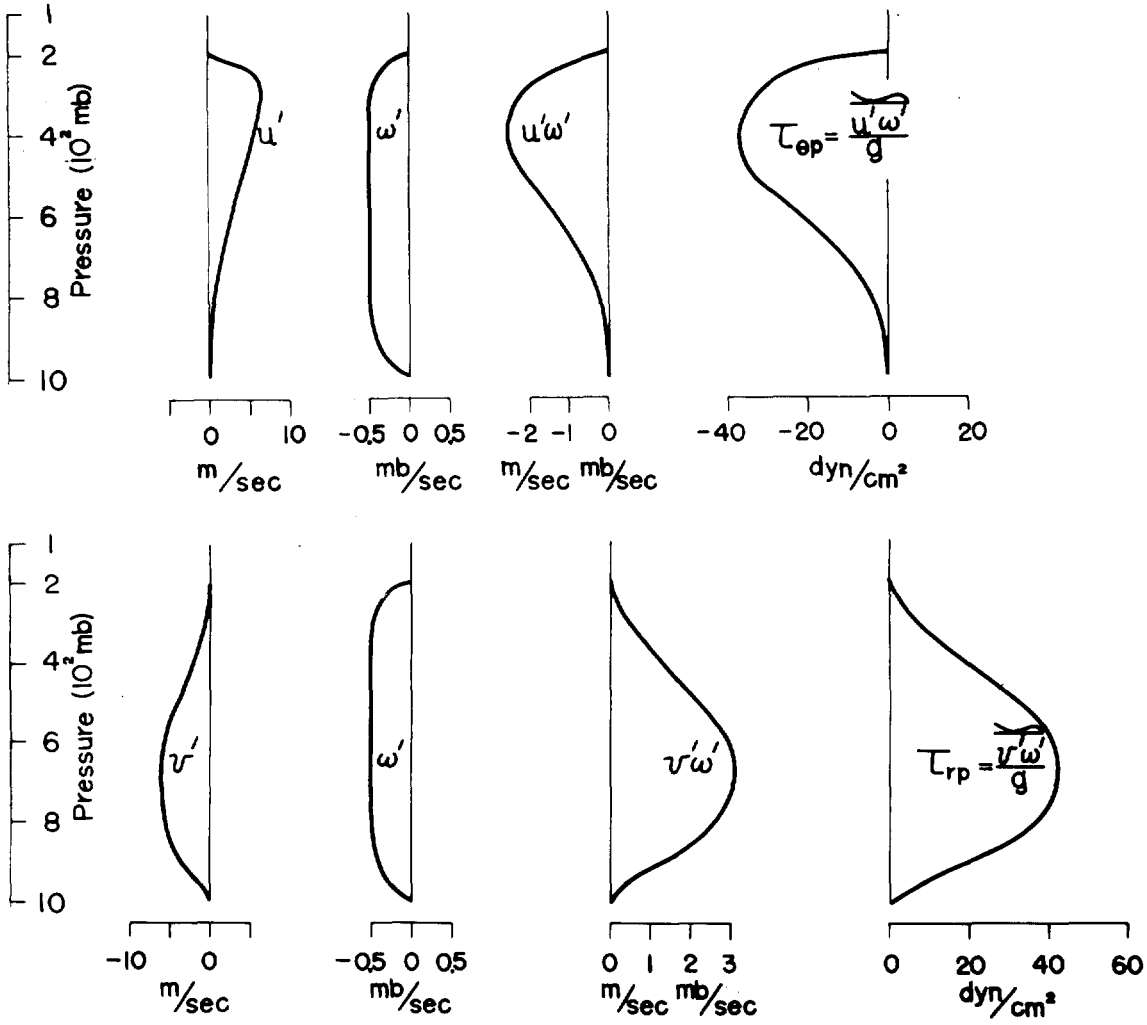

FIGURE 13.—Tropospheric distribution at 35-km. radius of the magnitude of the resulting assumed tangential (u'), radial (v'), and vertical (ω') wind eddies, their product, and consequent $\tau_{\theta p}$ and τ_{rp} stress which results from just the cumulonimbus updrafts if these components are correlated within the 15 percent area occupied by these updrafts.

$$v' = (v_i - \bar{v}) M_r \tag{17}$$

where v_i = the average radial wind in the lowest 50 mb.

$\bar{v}$ = the mean radial wind at each level,

M_r = radial mixing which is assumed to be proportional to cos φ instead of $\cos^{1/3} \varphi$ as with the tangential eddy,

φ = similar values for the five classes of cumulus up- and downdrafts as were specified for the tangential eddy wind.

Figure 12 and lower left-hand diagram of figure 13 portray the magnitude of radial eddy wind which would result from a cumulonimbus updraft through application of equation (17).

7. RESULTING CUMULUS-INDUCED STRESS AND HORIZONTAL ACCELERATION OF ASSUMED VORTEX

With the above-specified eddy winds, significantly large middle-level Reynolds stress values

$$\tau_{\theta p} = \frac{\widetilde{u'\omega'}}{g}, \qquad \tau_{rp} = \frac{\widetilde{v'\omega'}}{g}, \tag{18}$$

(where $\simeq$ denotes horizontal space averaging over distances considerably larger than the eddy) are present when the eddy wind components are appreciably correlated.[8] These stress magnitudes may be as large as the surface interface stress. Figure 13 portrays the specified vertical distribution u', v', and ω' wind eddies from the cumulonimbi updrafts at 35-km. radius and the resulting Reynolds stress which would result from the correlation of the horizontal and vertical eddies within 15 percent of the area which is occupied by Cb updrafts at the eye wall.

It is assumed in this model that in the first approximation to the turbulent stress there is complete correlation of wind eddies within the restricted areas of the cumulus elements and no correlation of wind eddies within the

[8] See Gray [14] for a discussion of the treatment of cumulus-scale wind fluctuations as wind eddies from the Reynolds stress point of view.

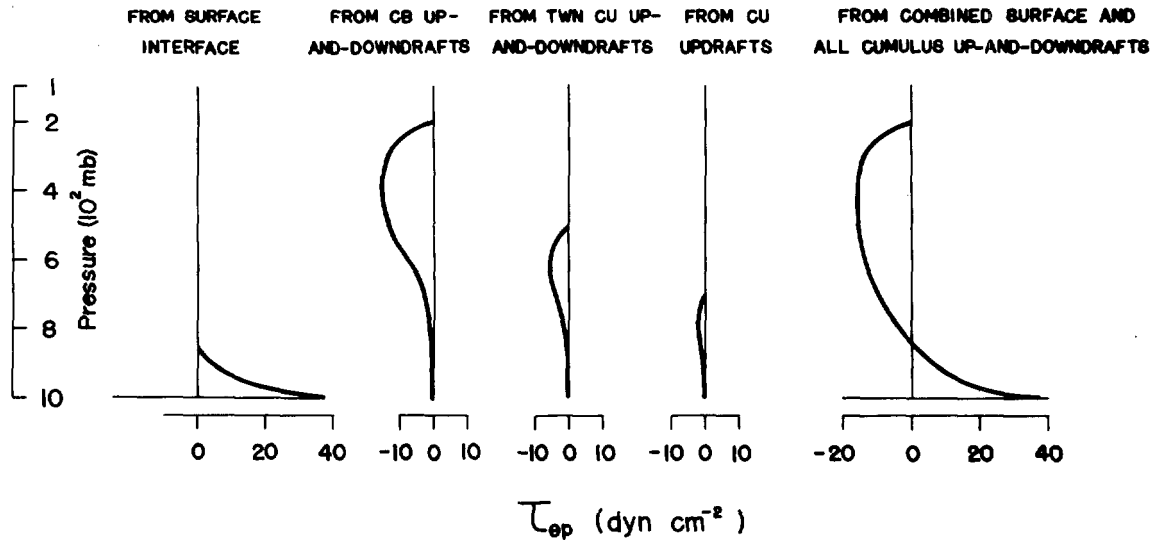

FIGURE 14.—Tropospheric distribution of average $\tau_{\theta p}$ stress between radii 30 and 50 km. (right diagram) which results from the combined surface interface stress (left diagram) and the three sizes of cumuli (center diagrams).

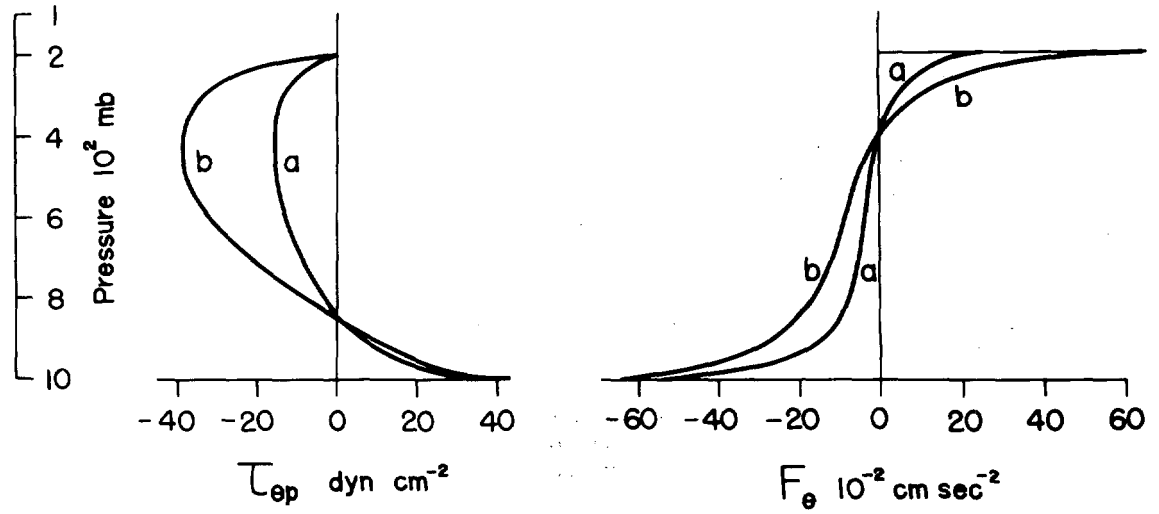

FIGURE 15.—Tropospheric distribution of $\tau_{\theta p}$ stress (left diagram) for average conditions between 30- and 50-km. radii (a), plus the value at 35-km. radius (b), and the resulting tangential frictional acceleration (F_θ) at these radii (right diagram).

much larger percentage areas with no cumuli. This is a different type of turbulence than the typical mechanically produced gust-turbulence of the planetary boundary layer. The typical eddies in this kind of cumulus-produced turbulence are much larger and are driven by the condensation-developed buoyancy within the selective cumulus draft. The author has, in fact, measured this latter type of turbulence from the U.S. Weather Bureau's specially instrumented aircraft observations in the hurricane. Draft-scale wind components often showed large correlation at selective regions within and surrounding the cumuli. Middle tropospheric stress values as high as 20–30 dynes/cm.^{2} were computed from the high correlation and magnitude of the draft-scale eddies within and surrounding the selective regions occupied by the cumuli. This scale of eddy was not observed in the cumulus-free areas. The reader is referred to the author's other paper [14] for a discussion of this latter type of turbulence.

$\tau_{\theta p}$ STRESS

The three center diagrams of figure 14 portray the vertical distribution of the average $\tau_{\theta p}$ stress between 30 and 50 km. which results from the up- and downdrafts within the three assumed classes of cumuli. The drawing on the left of figure 14 portrays the assumed vertical decrease of surface stress ($\tau_{\theta p}$). The drawing on the right of figure 14 shows the average stress between 30 and 50 km. which results from the combined surface and all three sizes of cumuli. In the surface boundary layer tangential momentum is being transferred downward by gust-scale eddies and $\omega' u'$ is positive. Malkus and Riehl [28], Riehl and Malkus [42], and Miller [32] have estimated hurricane boundary layer stress values of 40–60 dynes/cm.^{2} at inner radii. In the inflow layer where momentum is being transferred to the ocean, the eddy sizes are characteristically of gust length ($\sim$100 to 400 m.). Negative correlation between the vertical and

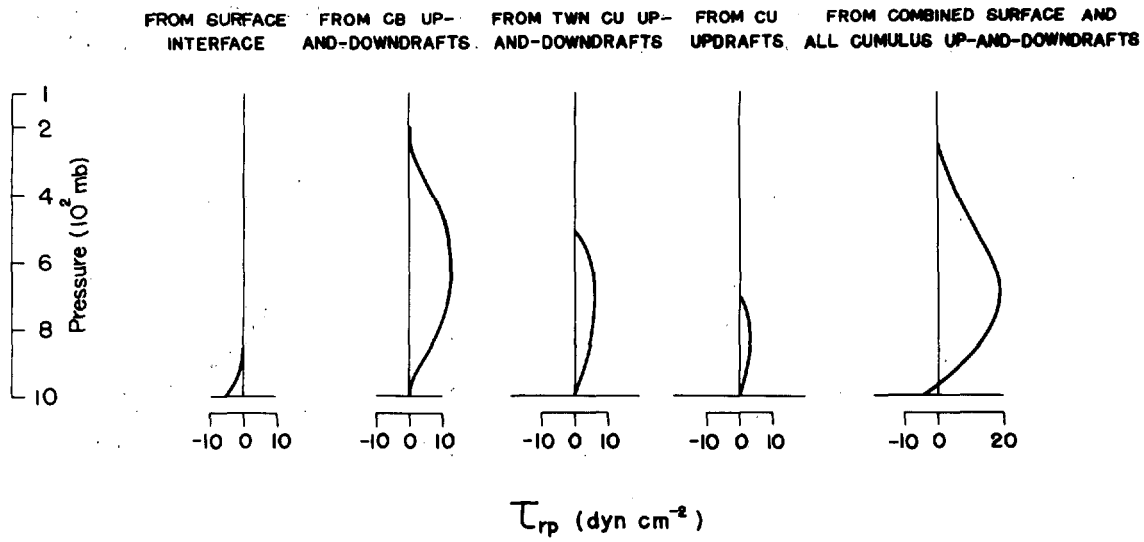

FIGURE 16.—Tropospheric distribution of average τ_{rp} stress between radii 30 and 50 km. (right diagram) which results from the combined surface interface stress (left diagram) and the three sizes of cumuli (center diagrams).

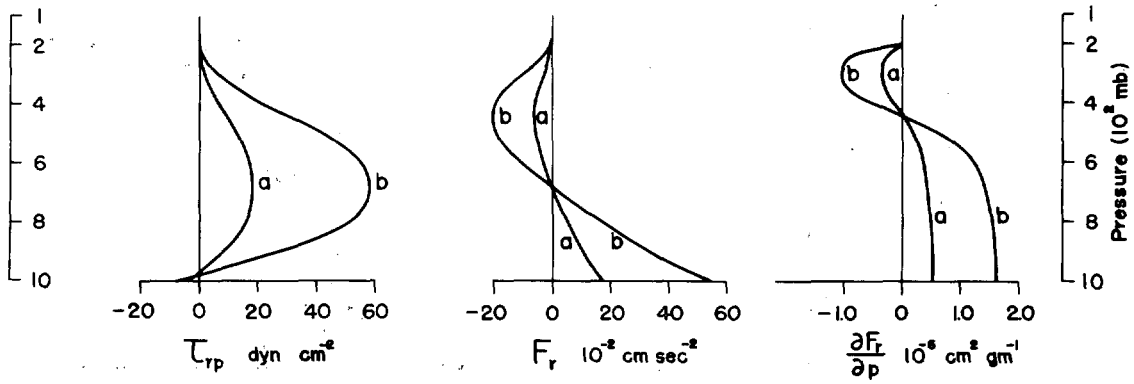

FIGURE 17.—Tropospheric distribution of τ_{rp} stress for average conditions between 30- and 50-km. radii (a) plus the value at 35-km. radius (b) is shown in the drawing on the left. Resulting distributions of radial frictional acceleration (F_r) and vertical gradient of radial acceleration $\partial F_r/\partial p$ at these same radii are shown in the center and right drawings, respectively.

horizontal gust eddies is required for momentum transfer to the ocean surface. The few B–50 flights at 450 m. height that have been made in strong wind conditions have ususally encountered a mechnical "washboard" type of turbulence. U.S. Navy flights at sub-cloud levels in typhoons have also reported this type of turbulence. Beginning at cloud base (400 to 600 m.) and extending into the upper troposphere, a characteristically different type of "cumulus-scale" eddy wind turbulence is established. In this case momentum is being transferred upward by the positive correlation of cloud-scale tangential and vertical eddies. These eddies are typically of much longer size than the eddies within the surface inflow layer.

TANGENTIAL ACCELERATION (F_θ)

The left diagram of figure 15 shows the vertical distribution of the average combined $\tau_{\theta p}$ stress within the 30–50-km. radii, (a), and the $\tau_{\theta p}$ stress which occurs at the eye wall at 35 km., (b). A larger magnitude of stress exists at the eye-wall where the intensity of cumulus convection is greatest. The right diagram shows the tangential frictional acceleration (F_θ) which results between and at these same radii from the vertical gradient of this combined $\tau_{\theta p}$ stress.[9] It is to be noted that significant tangential accelerations occur in the middle and upper troposphere and that these accelerations are of a sign such that they act to suppress the tropospheric wind shear.

τ_{rp} STRESS

The right diagram of figure 16 shows the combined stress resulting from the surface interface (left diagram) and τ_{rp} stress induced by the three sizes of cumuli. It is to be noted that the level of largest τ_{rp} stress is 700 mb. instead of near 400 mb. as in the case of $\tau_{\theta p}$. This is due to the larger vertical shear of $\bar{v}$ at the lower levels. τ_{rp} at the surface is taken to be equal to $(\bar{v}/\bar{u})\tau_{\theta p}$. Over the tropical oceans and in hurricanes, cumulus clouds extend upward from a base of about 50–60 mb. above the ocean

[9] In an earlier study (Gray [14]) it was shown that the vertical gradient of stress was the predominant contributor to horizontal accelerations. Horizontal gradients of stress contributed in an insignificant way to horizontal acceleration.

surface. From the surface inflow layer, a large export of inward radial momentum must take place both to the sea surface and also upward within the cumulus cloud. The downdrafts from above which penetrate into the inflow layer carry a smaller inward radial momentum component with them and add to this export. These vertical exchanges of radial momentum induce a sizable vertical gradient of τ_{rp} stress.

RADIAL ACCELERATION (F_r) AND $\partial F_r/\partial p$

Figure 17 is similar to figure 15. The left diagram portrays the vertical distribution of the average combined τ_{rp} stress within 30–50-km. radii, (a), and the τ_{rp} stress occurring at the eye wall at 35-km. radius, (b). The center diagram shows the resulting frictional acceleration (F_r) obtained from the vertical gradient of this stress. F_r is directed so as to inhibit the mass circulation through the vortex. An excess of pressure over wind acceleration then becomes a necessary requirement for maintenance of the mass circulation through the system.

The diagram on the right of figure 17 shows the vertical gradient of F_r (i.e., $\partial F_r/\partial p$) in units of 10^{-6} cm.^{2} gm.$^{-1}$ These are the same units used for the measured B_{ex} of table 8. The average observed value of B_{ex} as shown in table 8 for radii between 18 and 54 km. is 1.7×10^{-6} cm.^{2}/gm. The calculated values of $\partial F_r/\partial p$ in the lower third of the troposphere shown in the right diagram of figure 17 are 0.5 and 1.5×10^{-6} cm.^{2}/gm. for average conditions between 30 and 50 km. and at 35 km., respectively. These computed values are of the right sign and magnitude to offer a plausible explanation for the large observed B_{ex}. It is thus concluded that the $\partial F_r/\partial p$ term of (3) is always of very large magnitude at the inner areas of the typical hurricane and can, in fact, *account for most of the continuous steady-state imbalance of wind and pressure acceleration.* The magnitude of the $\partial(\partial\bar{u}/\partial t)/\partial p$ term of (3) must be small in comparison to $\partial F_r/\partial p$ if unreasonably large growth rates are not to occur. The magnitude of the $\partial(\bar{v}\partial\bar{v}/\partial r)/\partial p$ and $\partial(\bar{\omega}\partial\bar{v}/\partial p)/\partial p$ terms of (3) is also smaller above the surface inflow layer ($p<850$ mb.).

Given the lower stratospheric boundary condition of no pressure and wind gradient, a downward integration of $\partial F_r/\partial p$ through the troposphere produces the largest B_{ex} at the surface as shown in figure 18. This is produced primarily by the imbalance of the thermal-wind equation. Negative B_{ex} and stronger wind than pressure acceleration is hypothesized to be present above 450 mb. Below 450 mb. B_{ex} is positive and the pressure acceleration is stronger than wind acceleration.

A much larger pressure than wind acceleration is required in the lowest layer to maintain a continual inward acceleration of the surface wind in order to balance the continual drain of inward-directed radial momentum to the ocean surface below and by the cumuli above (fig. 5). An excess of heating and pressure acceleration over wind acceleration must always be present within the steady-state storm to maintain this inflow. The observations of

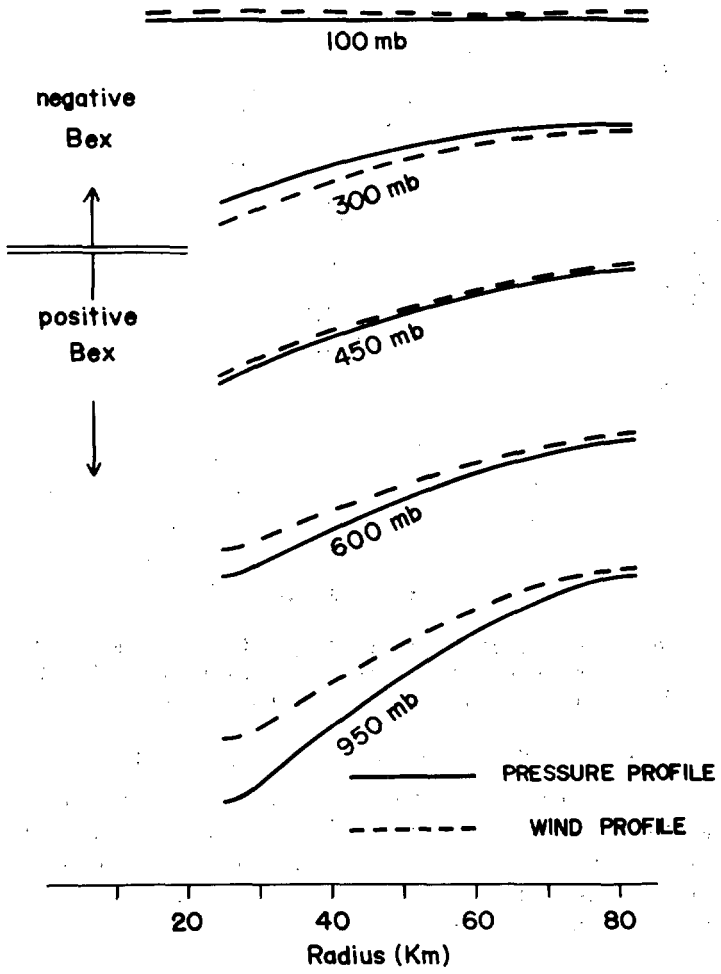

FIGURE 18.—Comparison of the unbalanced pressure and wind (converted into equivalent pressure gradient) profiles at various levels in the assumed steady-state vortex.

Graham and Hudson [11] and Schauss [46] have shown sizably larger cyclostrophic (or pressure gradient) than observed wind at the surface levels of the hurricane. In an earlier study the author found an excess of vortex averaged pressure over wind acceleration (Gray [12]). It is to be noted that the largest values of $\partial F_r/\partial p$ are found at the lowest level.

The cumuli produce the larger pressure gradients through condensation heating and also produce the mechansim whereby compensating radial accelerations are inhibited. In this way a steady-state imbalance of wind and pressure gradient can be maintained. The cumulus-induced radial accelerations act to inhibit compensating inward radial cross-isobaric motion which would generate large amounts of kinetic energy in the manner discussed by Palmén and Jordan [37].

In the tangential direction the cumulus momentum exchanges also act to inhibit a larger generation of wind at the lowest levels. It is then possible for the inward directed cross-isobaric flow, both in the steady-state and intensifying vortex case, to be larger at the lowest levels, yet for the vertical gradient of horizontal wind to remain small.

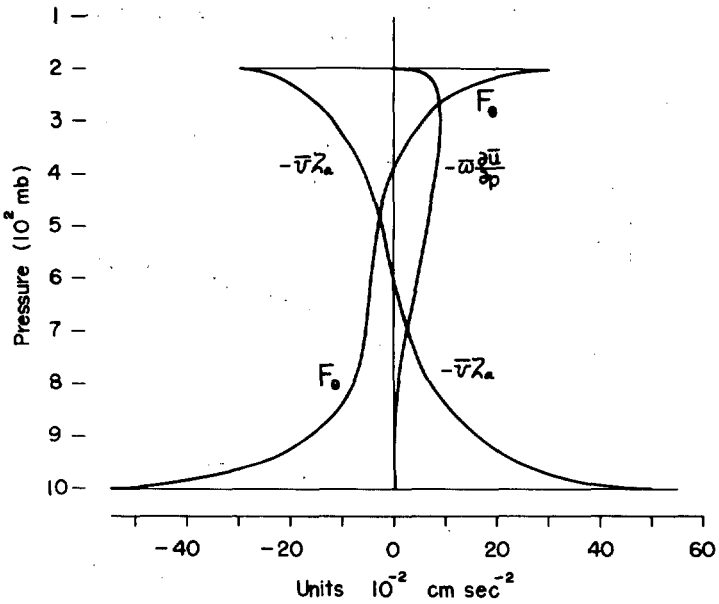

FIGURE 19.—Tropospheric distribution of the magnitudes of the three terms in the steady-state tangential equation of motion which have been averaged between radii 30 and 50 km.

STEADY-STATE TANGENTIAL EQUATION OF MOTION

As a check on the balance of accelerations and the significance of the cumulus-induced accelerations, an examination was made of the terms in the symmetrical steady-state tangential equation of motion. This equation may be written as

$$0=-\bar{v}\zeta_a-\bar{\omega}\frac{\partial\bar{u}}{\partial p}+F_\theta \tag{19}$$

Figure 19 shows the 30–50-km. radial average of the vertical variation of these three terms for conditions of the assumed vortex with the superimposed cumulus convection. It is again seen that a sizable magnitude of F_θ must prevail through the middle and upper troposphere in order that balance prevail. It is impossible to prescribe a steady vortex with radial inflow near the surface and outflow concentrated at 200 mb. without simultaneously prescribing a vertical distribution of frictional acceleration similar to figure 19 (with small $\bar{\omega}\partial\bar{u}/\partial p$). The magnitude and density of cumulus convection chosen were such as to just allow for balanced conditions. A balance of momentum is also prescribed by conditions of equation (19).

The magnitude of the cumulus downdrafts has been conservatively chosen to be but one-half that of the updrafts and to exist only within the lower half of the troposphere. With this specification the relative magnitude of $|F_\theta|$ to $|\bar{\omega}\partial\bar{u}/\partial p|$ through the troposphere is approximately three to one. A smaller updraft to downdraft ratio would make the above ratio considerably larger.

8. TANGENTIAL EQUATION FOR INTENSIFYING VORTEX

The symmetric cylindrical tangential equation for intensification is written as

$$\frac{\partial u}{\partial t}=-v\zeta_a-\omega\frac{\partial u}{\partial p}+F_\theta \tag{20}$$

Differentiating this partially with respect to pressure, we obtain

$$\frac{\partial}{\partial t}\left(\frac{\partial u}{\partial p}\right)=-\frac{\partial}{\partial p}(v\zeta_a)-\frac{\partial}{\partial p}\left(\omega\frac{\partial u}{\partial p}\right)+\frac{\partial F_\theta}{\partial p} \tag{21}$$

In the intensifying vortex there is little change of vertical shear in the lower half of the troposphere, and $\partial(\partial u/\partial p)/\partial t \sim 0$. The pressure gradient and inward radial velocity must be larger in the lower levels of the intensifying vortex. The vertical distribution of ζ_a and v requires that $-\partial(v\zeta_a)/\partial p$ be positive. $\partial(\partial u/\partial p)/\partial t$ can remain small only by $-\partial(\omega\partial u/\partial p)/\partial p$ and $\partial F_\theta/\partial p$ contributing in a negative sense to balance $-\partial(v\zeta_a)/\partial p$. In this way it is possible for the absolute vorticity and vertical gradient of radial wind to increase in the lower half of the troposphere but for the vertical gradient of tangential speed to remain small. It is to be noticed (fig. 19) that in the lower half of the troposphere the ∂F_θ term resulting from the cumulus up- and downdrafts is of much larger magnitude than the $\bar{\omega}\partial\bar{u}/\partial p$ term.

9. OTHER CONSIDERATIONS

With characteristic cumulus-induced stress as previously discussed, resulting values of vertical and horizontal kinematic eddy viscosity can range as high as 10^9 cm.^{2}/sec. Figure 20 portrays the vertical distribution of kinematic viscosity (ν) coefficients (in units of 10^7 cm.^{2}/sec.) which are defined as

$$\nu\ (\text{vertical})=\left|\frac{\tau_{\theta p}}{\rho^2 g\dfrac{\partial\bar{u}}{\partial p}}\right|,\qquad \left|\frac{\tau_{rp}}{\rho^2 g\dfrac{\partial\bar{v}}{\partial p}}\right| \tag{22}$$

and are required with the various calculated values of stress and mean wind shear. A wide range and large magnitude of kinematic viscosity is required to satisfy conditions of the assumed vortex. This is particularly true at middle tropospheric levels in the cases where τ_{rp} is large and the shear of the mean radial wind small. The magnitude of kinematic viscosity can range from one to three orders of magnitude greater than the values which have been generally used in the previously cited numerical experiments. It would appear that the usually assumed mixing length theory which equates the magnitude of stress proportional to the mean shear (although relatively valid for the usual mechanical gust-scale mixing occurring in the atmosphere's surface layers) is not valid for fluid mixing accomplished by cumulus clouds where thermodynamic changes also occur. Attempts to account for the turbulent mixing by the cumuli in terms of mean shearing conditions appear not to be realistically valid.

Eddy momentum exchange coefficients characteristic of these higher magnitudes might shift the most preferred growth scale of cumulus-induced heating away from the cumuli to the more realistic mesoscale and offer a physical

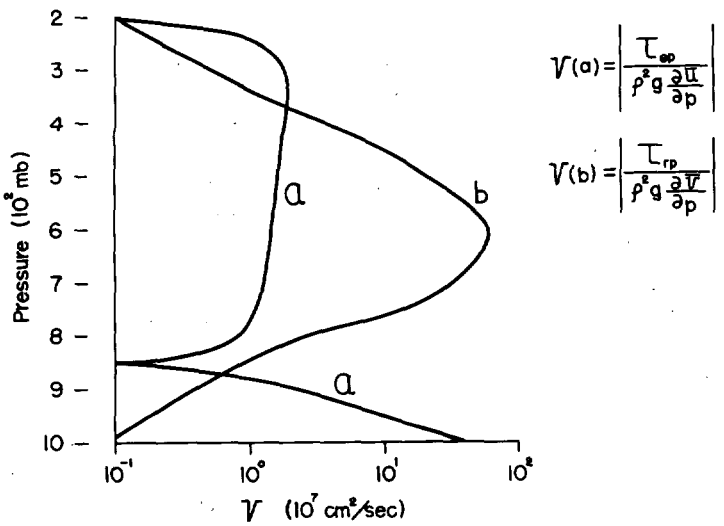

FIGURE 20.—Average vertical kinematic eddy viscosity coefficients (ν) between 30- and 50-km. radii which would result from stress and mean wind shears of assumed vortex. Units: 10^7 cm.^{2}/sec.

explanation of how the cumulus clouds on a scale of 1–10 km. can generate a system which is two orders of magnitude larger. The buoyancy-produced draft-scale eddy with a lifetime of but 10–15 min. rapidly generates smaller turbulence eddies on its boundaries. These smaller gust-scale eddies act to diffuse the heat and momentum of the draft eddy away from the cumuli to the larger system. This heat and momentum diffusion is viewed as occurring at a faster rate than that at which the cumulus-induced pressure gradients from the condensation heat are able to concentrate a separate cumulus-scale velocity system of their own. But the condensation heat is not lost. It remains within the larger system to maintain and intensify it. The momentum exchanges, on the other hand, do not accumulate and vanish or remain in direct relation to the continuance of the cumulus intensity and shearing flow.

10. SUMMARY DISCUSSION

The vertical momentum transports associated with cumulus up- and downdrafts offer a physical explanation for the observed 200 to 300 percent excess baroclinicity in the inner areas of the hurricane. These transports allow a steady-state vortex imbalance of wind and pressure acceleration. They allow maintenance of a vortex in which the in- and outflow is predominantly concentrated in the lower and upper troposphere. They offer a mechanism whereby the upper and lower tropospheric circulations can be coupled, and explain how vertical wind shear can remain small as baroclinicity increases. They further open up the possibility that cumulus momentum exchanges can act as a basic mechanism for the generation of tropical easterly waves and other phenomena.

The alteration of wind and pressure in response to cumulus condensation need not take place simultaneously. Condensation heat must initially go directly to lower the pressure surfaces (with assumed upper boundary) and increase the horizontal pressure and temperature gradients. Very little is known about the resulting time-dependent adjustment of the wind changes in the real atmosphere. Adjustment solutions and discussions (Rossby [45], Cahn [6], Bolin [3], Washington [55]) have been made only under highly idealized conditions. Numerical experiments should be undertaken to learn more of the details of the adjustment processes in the cumulus atmosphere. It is further suggested that future numerical experiments which incorporate cumulus convection should also include the effects of cloud-scale momentum transports in addition to the effects of condensation heat.

It is important to appreciate the physical significance of cumulus-scale vertical momentum transports and of the dual or "paradox" role which the cumuli can play. It is hypothesized that if the cumulus-induced baroclinicity in the lower half of the troposphere were to act in the usual sense to increase the wind shear, the development of the tropical wave and vortex could not proceed. Increased vertical wind shear would create an environment less conducive to further cumulus development (Asai [2], Hitschfeld [18], Malkus and Scorer [27]). The increased vertical shear would prevent concentration of temperature.

The above ideas are a further extension of the so-called "hot tower" hypothesis of Malkus [30] and Riehl and Malkus [41], [42], who emphasized the importance of selective vertical transport of heat within the cumulus up- and downdraft. In addition to the transport of heat, this paper has emphasized the fundamental importance of vertical transport of momentum by the cumuli.

APPENDIX

Accuracy of Data. For information concerning the accuracy of the flight observations the reader is referred to the previously cited references on the Research Flight Facility (RFF) instrumentation. Strong evidence points to the basic reliability of the instruments, and especially to measured parameters which have been averaged over time and space such as the 18-km. vortex averages of wind and temperature. Navigation corrections after a number of hours of flight with the measured winds were usually within a few kilometers. When averaging was accomplished over the radial intervals at two levels, there was usually close hydrostatic consistency between the measured temperature gradients and the gradients of layer thickness. Although some observational and computational shortcomings may be present it is not thought possible that they could be of such an extent as to alter the conclusions or implications which are advanced. Choice of a larger or smaller smoothing interval for determining the radial temperature gradients would likewise not significantly affect the results.

Correction of Winds Computed from Doppler Navigation System. The Doppler Navigation system allows computa-

242-850 O—67——2

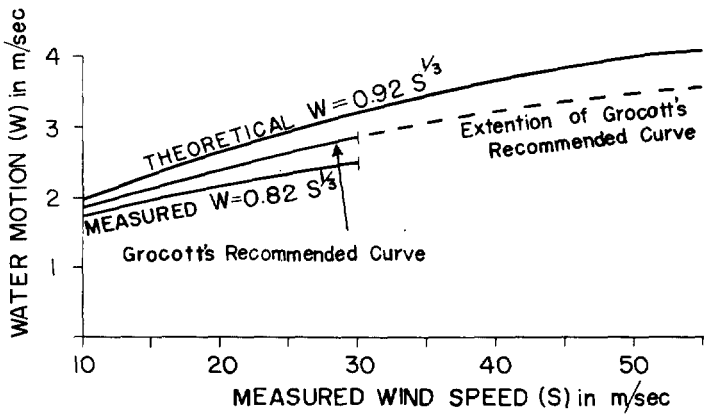

FIGURE 21.—Regression curve for Doppler determined wind speed vs. water motion for theoretical and for Grocott's [15] measured and recommended values.

tion of wind velocity from the vector difference of the true airspeed and the aircraft motion relative to the ocean surface. It is reasonable that small percentage errors might occur in the wind determination if wind-driven ocean particle motion is present. Because of the difficulties of precise testing of this effect in hurricanes, no determination has yet been made of the small percentage correction which should be applied to the winds.

Quantitative information concerning this likely effect has however been gathered by a British Royal Air Force group (Grocott [15]) in wind conditions up to 30 m./sec. over the North Atlantic.

Individual surface particles which reflect the electromagnetic energy for the Doppler determination do not move at the same speed as surface waves. They describe circles whose radii decrease with increasing depth. Theoretically determined curves are available which relate the particle speed to wave length, wave height, and wave velocity. Observational relations of wave velocity to wind speed are also available. Combining these two relationships, Grocott [15] presents an equation relating surface wind speed and surface ocean particle motion, thus

$$W=0.92\ S^{1/3}$$

where W=water particle motion in m./sec. and S=Doppler measured wind speed in m./sec.

This relationship is shown as the theoretical curve of figure 21 which has been extended up to wind speeds of 60 m./sec. Grocott also presents observationally determined water motion from a Doppler system which was obtained from flight navigation corrections. For wind speeds up to 30 m./sec. he found the relationship $W=0.82\ S^{1/3}$. Considering all aspects Grocott recommends use of a curve ($W=0.87\ S^{1/3}$) which is intermediate between measured and theoretically determined values. Grocott's recommended curve has been extended for this study to include wind speeds above 30 m./sec. although it is uncertain that the functional dependence may not be altered at the higher wind speeds in tropical storms.

The Doppler correction of $W=0.87\ S^{1/3}$ requires an increase of the measured RFF winds in the data presented from 7 to 9 percent. It seems reasonable that this effect would also occur with hurricane winds. To obtain the best possible winds it was deemed advisable to apply this correction. The results and implications of this paper are, however, in no significant way dependent on this correction's being applied. The observed thermal wind imbalance of 200 to 300 percent in the inner area of the hurricane would not be substantially affected by a 5–10 percent alteration of the wind speed.

ACKNOWLEDGMENTS

To Drs. M. Yanai and T. Matsuno of Tokyo University for critical reading of manuscript and discussion; to the National Hurricane Research Laboratory who supplied the valuable data used in this study. This research has been sponsored by the National Science Foundation under auspices of the U.S.-Japan Cooperative Science Program and was performed while the author was in Tokyo.

REFERENCES

1. B. Ackerman, "Some Observations of Water Contents in Hurricanes," *Journal of the Atmospheric Sciences*, vol. 20, No. 4, July 1963, pp. 288–298.
2. T. Asai, "Cumulus Convection in the Atmosphere With Vertical Wind Shear: Numerical Experiment," *Journal of Meteorological Society of Japan*, Ser. 2, vol. 42, No. 4, Aug. 1964, pp. 245–259.
3. B. Bolin, "The Adjustment of a Nonbalanced Velocity Field Towards Geostrophic Equilibrium in a Stratified Fluid," *Tellus*, vol. 5, No. 3, Aug. 1953, pp. 373–385.
4. H. R. Byers and R. R. Braham, *The Thunderstorm*, U.S. Weather Bureau, 1949, 287 pp.
5. H. R. Byers and L. J. Battan, "Some Effects of Vertical Wind Shear on Thunderstorm Structure," *Bulletin of the American Meteorological Society*, vol. 30, No. 5, May 1949, pp. 168–175.
6. A. Cahn, Jr., "An Investigation of the Free Oscillations of a Simple Current System," *Journal of Meteorology*, vol. 2, No. 2, June 1945, pp. 113–119.
7. J. G. Charney and A. Eliassen, "On the Growth of the Hurricane Depression," *Journal of the Atmospheric Sciences*, vol. 21, No. 1, Jan. 1964, pp. 68–75.
8. J. A. Colón and Staff NHRP, "On the Structure of Hurricane Daisy (1958)," *National Hurricane Research Project Report* No. 48, U.S. Weather Bureau, 1961, 102 pp.
9. J. A. Colón and Staff NHRP, "On the Structure of Hurricane Helene (1958)," *National Hurricane Research Project Report* No. 72, U.S. Weather Bureau, 1964, 56 pp.
10. R. C. Gentry, "A Study of Hurricane Rainbands," *National Hurricane Research Project Report* No. 69, U.S. Weather Bureau, 1964, 85 pp.
11. H. E. Graham and G. N. Hudson, "Surface Winds Near the Center of Hurricanes (and Other Cyclones)," *National Hurricane Research Project Report* No. 39, U.S. Weather Bureau, 1960, 200 pp.
12. W. M. Gray, "On the Balance of Forces and Radial Accelerations in Hurricanes," *Quarterly Journal of the Royal Meteorological Society*, vol. 88, No. 378, Oct. 1962, pp. 430–458.
13. W. M. Gray, "Calculations of Cumulus Vertical Draft Velocities in Hurricanes from Aircraft Observations," *Journal of Applied Meteorology*, vol. 4, No. 4, Aug. 1965, pp. 463–474.
14. W. M. Gray, "On the Scales of Motion and Internal Stress Characteristics of the Hurricane," *Journal of the Atmospheric Sciences*, vol. 23, No. 3, May 1966, pp. 278–288.
15. D. F. Grocott, "Doppler Correction for Surface Movement," *Journal of Instrument Navigation*, vol. 16, 1963, pp. 57–63.
16. H. F. Hawkins, F. E. Christensen, S. C. Pearce, and Staff NHRP, "Inventory, Use, and Availability of National Hurricane Research Project Data Gathered by Aircraft," *National*

Hurricane Research Project Report No. 52, U.S. Weather Bureau, 1962, 240 pp.
17. H. F. Hawkins, "Vertical Wind Profiles in Hurricanes," *National Hurricane Research Project Report* No. 55, U.S. Weather Bureau, 1962, 16 pp.
18. W. Hitschfeld, "The Motion and Erosion of Convective Storms in Severe Vertical Wind Shear," *Journal of Meteorology*, vol. 17, No. 3, June 1960, pp. 270–282.
19. L. A. Hughes, "On the Low-Level Wind Structure of Tropical Storms," *Journal of Meteorology*, vol. 9, No. 6, Dec. 1952, pp. 422–428.
20. C. L. Jordan, "The Thermal Structure of the Core of Tropical Cyclones," *Geophysica*, vol. 6, No. 314, 1958, pp. 281–297.
21. C. L. Jordan, D. A. Hurt, Jr., and C. A. Lowrey, "On the Structure of Hurricane Daisy on 27 August 1958," *Journal of Meteorology*, vol. 17, No. 3, June 1960, pp. 337–348.
22. A. Kasahara, "A Numerical Experiment on the Development of a Tropical Cyclone," *Journal of Meteorology*, vol. 18, No. 3, June 1961, pp. 259–282.
23. A. Kasahara, "A Numerical Model of Tropical Cyclones," *Proceedings, Symposium on Tropical Meteorology, Rotorua, New Zealand, 1963*, New Zealand Meteorological Service, Wellington, 1964, pp. 650–659.
24. H. L. Kuo, "On Formation and Intensification of Tropical Cyclones Through Latent Heat Release by Cumulus Convection," *Journal of the Atmospheric Sciences*, vol. 22, No. 1, Jan. 1965, pp. 40–63.
25. N. E. LaSeur and H. F. Hawkins, "An Analysis of Hurricane Cleo (1958) Based on Data from Research Reconnaissance Aircraft," *Monthly Weather Review*, vol. 91, Nos. 10–12, Oct.–Dec. 1963, pp. 694–709.
26. J. S. Malkus, "The Slopes of Cumulus Clouds in Relation to External Wind Shear," *Quarterly Journal of the Royal Meteorological Society*, vol. 78, No. 338, Oct. 1952, pp. 530–542.
27. J. S. Malkus and R. S. Scorer, "The Erosion of Cumulus Towers," *Journal of Meteorology*, vol. 12, No. 1, Feb. 1955, p.p 43–57.
28. J. S. Malkus and H. Riehl, "On the Dynamics and Energy Transformation in Steady State Hurricanes," *Tellus*, vol. 12, No. 1, Feb. 1960, pp. 1–20.
29. J. S. Malkus et al., "Cloud Pattern in Hurricane Daisy, 1958," *Tellus*, vol. 13, No. 1, Feb. 1961, pp. 8–30.
30. J. S. Malkus, "Recent Developments in Studies of Penetrative Convection and an Application to Hurricane Cumulonimbus Towers," *Cumulus Dynamics, Proceedings, First Conference on Cumulus Convection, Wentworth, N. H., 1959*, Pergamon Press, New York, 1960, pp. 65–84.
31. B. I. Miller, "On the Momentum and Energy Balance of Hurricane Helene, (1958)," *National Hurricane Research Project Report* No. 53, U.S. Weather Bureau, 1962, 19 pp.
32. B. I. Miller, "On the Filling of Tropical Cyclones Over Land," *National Hurricane Research Project Report* No. 66, U.S. Weather Bureau, 1964, 82 pp.
33. C. W. Newton and H. R. Newton, "Dynamic Interactions Between Large Convective Clouds and Environment With Vertical Shear," *Journal of Meteorology*, vol. 16, No. 5, Oct. 1959, pp. 483–496.
34. C. W. Newton, "Dynamics of Severe Convective Storms," *Meteorological Monographs*, vol. 5, No. 27, American Meteorological Society, Boston, 1963, pp. 33–58.
35. Y. Ogura, "Frictionally Controlled, Thermally Driven Circulations in a Circular Vortex With Application to Tropical Cyclones," *Journal of the Atmospheric Sciences*, vol. 21, No. 6, Nov. 1964, pp. 610–621.
36. K. Ooyama, "A Dynamical Model for the Study of Tropical Cyclone Development," *Proceedings*, Third Technical Conference on Hurricanes and Tropical Meteorology, Mexico City, 1963.
37. E. Palmén and C. Jordan, "Note on the Release of Kinetic Energy in Tropical Cyclones," *Tellus*, vol. 7, No. 2, May 1955, pp. 186–188.
38. E. Palmén and H. Riehl, "Budget of Angular Momentum and Energy in Tropical Cyclones," *Journal of Meteorology*, vol. 14, No. 2, Apr. 1957, pp. 150–159.
39. C. Reber and H. Friedman, "Manual of Meteorological Instrumentation and Data Processing of the Research Flight Facility," U.S. Weather Bureau, 1964 (Available from U.S. Weather Bureau, Miami, Fla.).
40. H. Riehl, *Tropical Meteorology*, McGraw-Hill Book Co., Inc., New York, 1954, 392 pp.
41. H. Riehl and J. S. Malkus, "On the Heat Balance in the Equatorial Trough Zone," *Geophysica*, vol. 6, No. 3/4, 1958, pp. 503–538.
42. H. Riehl and J. S. Malkus, "Some Aspects of Hurricane Daisy, 1958," *Tellus*, vol. 13, No. 2, May 1961, pp. 181–213.
43. H. Riehl, "Some Relations Between Wind and Thermal Structure of Steady State Hurricanes," *Journal of the Atmospheric Sciences*, vol. 20, No. 4, July 1963, pp. 276–287.
44. S. L. Rosenthal, "Some Attempts to Simulate the Development of Tropical Cyclones by Numerical Methods," *Monthly Weather Review*, vol. 92, No. 1, Jan. 1964, pp. 1–21.
45. C.-G. Rossby, "On the Mutual Adjustment of Pressure and Velocity Distribution in Certain Simple Current Systems," *Journal of Marine Research*, vol. 1, 1938, pp. 239–263.
46. C. E. Schauss, "Reconstruction of Surface Pressure and Wind Fields of Hurricane Helene," *National Hurricane Research Project Report* No. 59, U.S. Weather Bureau, 1962, 46 pp.
47. H. V. Senn and E. F. Low, "Studies of the Evolution and Motion of Radar Echoes from Hurricanes," Unpublished Research Report of Marine Laboratory and Radar Research Laboratory, University of Miami, 1959, 109 pp. (ASTIA AD–227258).
48. H. V. Senn and H. W. Hiser, "On the Origin of Hurricane Spiral Rain Bands," *Journal of Meteorology*, vol. 16, No. 4, Aug. 1959, pp. 419–426.
49. H. V. Senn, H. W. Hiser, and E. F. Low, "Studies of the Evolution and Motion of Hurricane Spiral Bands from Hurricanes," Unpublished Research Report of Marine Laboratory and Radar Research Laboratory, University of Miami, Report No. 8924–1, 1959, 55 pp. (ASTIA AD–227258).
50. H. V. Senn, H. W. Hiser, and R. D. Nelson, "Studies of the Evolution and Motion of Radar Echoes from Hurricanes," Unpublished Research Report of Marine Laboratory and Radar Research Laboratory, University of Miami, Report No. 8944–1, 1960, 75 pp. (ASTIA AD–24979).
51. H. V. Senn, H. W. Hiser, and J. A. Stevens, "Radar Hurricane Research 1 July 1961 to 30 June 1962," Unpublished Research Report of Marine Laboratory and Radar Research Laboratory, University of Miami, Report No. 8858–1, 1961, 109 pp. (ASTIA AD–264959).
52. S. Syōno and R. Yamasaki, "Vertical Partition of Condensation Related to Tropical Storm Development," *Journal of Meteorological Society of Japan* vol. 44, 1966 (in press).
53. J. S. Simpson et al., "Experimental Cumulus Dynamics," *Reviews of Geophysics*, vol. 3, 1965, pp. 387–431.
54. P. Squires and J. S. Turner, "An Entraining Jet Model for Cumulonimbus Updraughts," *Tellus*, vol. 14, No. 4, Nov. 1962, pp. 422–434.
55. W. M. Washington, "A Note on the Adjustment Towards Geostrophic Equilibrium in a Simple Fluid System," *Tellus*, vol. 16, No. 4, Nov. 1964, pp. 530–533.
56. K. Watanabe, "Vertical Wind Distribution and Weather Echo, (in Case of Typhoon Situation)," *Proceedings of the 10th Weather Radar Conference*, 1963, pp. 222–227.
57. M. Yanai, "Formation of Tropical Cyclones," *Reviews of Geophysics*, vol. 2, No. 2, May 1964, pp. 367–414.

[Received September 19, 1966; revised December 5, 1966]